Check for updates

EurJIC
European Journal of Inorganic Chemistry

Research Article
doi.org/10.1002/ejic.202300732

Chemistry Europe
European Chemical Societies Publishing

www.eurjic.org

Reduced 2,2′-Bipyridine Lanthanide Metallocenes Provide Access to Mono-C_5Me_5 and Polyazide Complexes

Cary R. Stennett,[a] Joseph W. Ziller,[a] and William J. Evans*[a]

Exploration of the reduction chemistry of the 2,2′-bipyridine (bipy) lanthanide metallocene complexes $Cp^*_2LnCl(bipy)$ and $Cp^*_2Ln(bipy)$ ($Cp^* = C_5Me_5$) resulted in the isolation of a series of complexes with unusual composition and structure including complexes with a single Cp* ligand, multiple azide ligands, and bipy ligands with close parallel orientations. These results not only reveal new structural types, but they also show the diverse chemistry displayed by this redox-active platform. Treatment of $Cp^*_2NdCl(bipy)$ with excess KC_8 resulted in the formation of the mono-Cp* Nd(III) complex, $[K(crypt)]_2[Cp^*Nd(bipy)_2]$, **1**, as well as $[K(crypt)][Cp^*_2NdCl_2]$, **2**, and the previously reported $[K(crypt)][Cp^*_2Nd(bipy)]$. A mono-Cp* Lu(III) complex, $Cp^*Lu(bipy)_2$, **3**, was also found in an attempt to make $Cp^*_2Lu(bipy)$ from $LuCl_3$, 2 equiv. of KCp*, bipy, and K/KI. Surprisingly, the $(bipy)^{1-}$ ligands in neighboring molecules in the structure of **3** are oriented in a parallel fashion with intermolecular C···C distances of 3.289(4) Å, which are shorter than the sum of van der Waals radii of two carbon atoms, 3.4 Å. Another product with one Cp* ligand per lanthanide was isolated from the reaction of $[K(crypt)][Cp^*_2Eu(bipy)]$ with azobenzene, which afforded the dimeric Eu(II) complex, $[K(crypt)]_2[Cp^*Eu(THF)(PhNNPh)]_2$, **4**. Attempts to make **4** from the reaction between $Cp^*_2Eu(THF)_2$ and a reduced azobenzene anion generated instead the mixed-valent Eu(III)/Eu(II) complex, $[K(crypt)][Cp^*Eu(THF)(PhNNPh)]_2$, **5**, which allows direct comparison with the bimetallic Eu(II) complex **4**. Mono-Cp* complexes of Yb(III) are obtained from reactions of the Yb(II) complex, $[K(crypt)][Cp^*_2Yb(bipy)]$, with trimethylsilylazide, which afforded the tetra-azido $[K(crypt)]_2[Cp^*Yb(N_3)_4]$, **6**, or the di-azido complex $[K(crypt)]_2[Cp^*Yb(N_3)_2(bipy)]$, **7a**, depending on the reaction stoichiometry. A mono-Cp* Yb(III) complex is also isolated from reaction of $[K(crypt)][Cp^*_2Yb(bipy)]$ with elemental sulfur which forms the mixed polysulfido Yb(III) complex $[K(crypt)]_2[Cp^*Yb(S_4)(S_5)]$, **8a**. In contrast to these reactions that form mono-Cp* products, reduction of $Cp^*_2Yb(bipy)$ with 1 equiv. of KC_8 in the presence of 18-crown-6 resulted in the complete loss of Cp* ligands and the formation of $[K(18\text{-}c\text{-}6)(THF)][Yb(bipy)_4]$, **9**. The $(bipy)^{1-}$ ligands of **9** are arranged in a parallel orientation, as observed in the structure of **3**, except in this case this interaction is intramolecular and involves pairs of ligands bound to the same Yb atom. Attempts to reduce further the Sm(II) $(bipy)^{1-}$ complex, $Cp^*_2Sm(bipy)$ with 2 equiv. of KC_8 in the presence of excess 18-crown-6 led to the isolation of a Sm(III) salt of $(bipy)^{2-}$ with an inverse sandwich Cp* counter-cation and a co-crystallized K(18-c-6)Cp* unit, $[K_2(18\text{-}c\text{-}6)_2Cp^*]_2[Cp^*_2Sm(bipy)]_2\cdot[K(18\text{-}c\text{-}6)Cp^*]$, **10**.

Introduction

Redox-active ligands have been used extensively in inorganic chemistry in order to effect chemical transformations that might otherwise be inaccessible to the metal being studied.[1–9] 2,2′-Bipyridine is one such ligand that can adopt three different oxidation states: the neutral species, bipy, and the anions $(bipy)^{1-}$ and $(bipy)^{2-}$. As such bipy has been employed to accomplish many different types of reactivity in concert with many elements across the periodic table. Early work with rare-earth elements described the unusual physical properties that can ensue in complexes binding radical bipy anions.[10–13] More recently, extensive studies by several groups have successfully used bipy and similar ligands to bring new coordination chemistry and new types of redox activity to the lanthanides and actinides.[14–22] We have recently found that bipy provides a facile high yield synthetic route, Scheme 1, to organometallic lanthanide metallocenes that function as monometallic two-electron reducing agents.[23]

Specifically, one-pot reactions of $LnCl_3$, KCp* ($Cp^* = C_5Me_5$) and bipy were shown to form $Cp^*_2LnCl(bipy)$. These complexes can be reduced by either one electron to afford $Cp^*_2Ln(bipy)$ or by two electrons to give $[Cp^*_2Ln(bipy)]^{1-}$ where the oxidation state of the bipy ligand in these complexes depends upon the specific lanthanide. The chemistry of $Cp^*_2Yb(bipy)$ and related systems was thoroughly investigated by Andersen to show that these complexes can possess multiconfigurational ground states and are thus more complicated than what is implied by assigned oxidation states.[24] Nevertheless, these $[Cp^*_2Ln(bipy)]^{1-}$ complexes can function as monometallic two-electron reductants, as demonstrated by their reactivity with substrates such as azobenzene or elemental sulfur to generate products with $(Ph_2N_2)^{2-}$ or $(S_5)^{2-}$ ligands, respectively, Scheme 2.

Although the reactions in Scheme 2 are stoichiometrically reasonable two-electron reductions, we have since found that other reactions of bipy metallocene complexes can generate unexpected products which are unusual in both composition and structure. Here, we report the X-ray crystal structures of these compounds to establish the existence of these structural

---

[a] C. R. Stennett, J. W. Ziller, W. J. Evans
Department of Chemistry, University of California, Irvine, California 92697, United States
E-mail: wevans@uci.edu

Supporting information for this article is available on the WWW under https://doi.org/10.1002/ejic.202300732

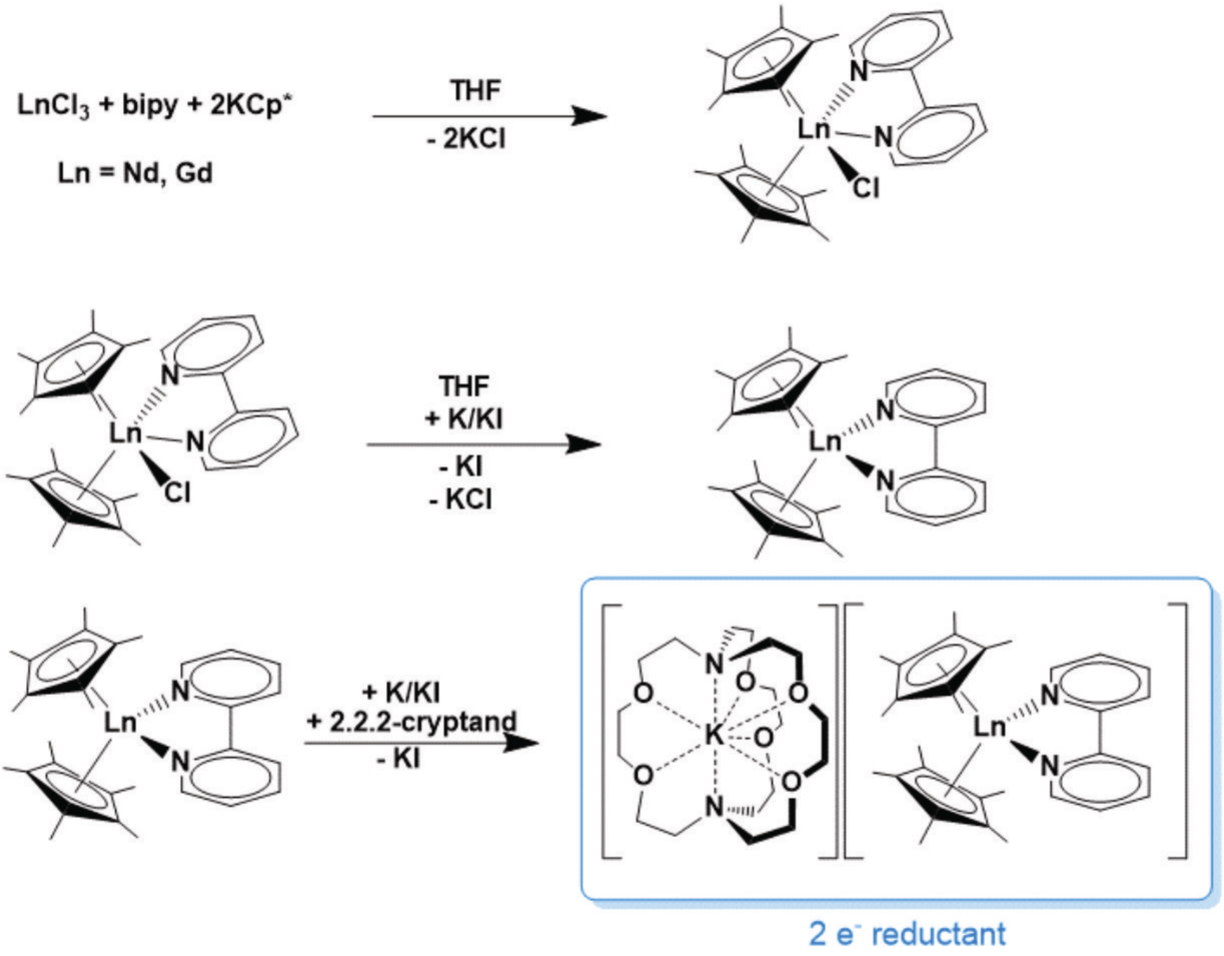

Scheme 1. Synthetic route to rare-earth monometallic two-electron reductants.

types and to show the unexpected chemistry that can be accessed via this redox-active bipy metallocene platform.

In general, these bipy metallocene reactions frequently form products containing just a single Cp* ligand per metal. Mono-Cp* lanthanide complexes are much less common than bis-Cp* compounds because the latter are more sterically saturated and tend to be more stable.[25] As pointed out in a comprehensive review on mono(cyclopentadienyl) complexes of rare-earth elements, the facile ligand redistribution that often occurs with the ionic lanthanides frequently leads to the more stable bis(cyclopentadienyl) complexes.[25] As a result, complexes such as $Cp^*LnA_2L_x$ and $(Cp^*LnA_3L_x)^{1-}$ (A = anion; L = neutral ligand; x = 0–3) have been much less studied than the metallocenes like $Cp^*_2LnAL_x$ and $(Cp^*_2LnA_2L_x)^{1-}$. As described in the review, “methods of synthesis somewhat more sophisticated than the usual salt metathesis are commonly employed” to make mono(cyclopentadienyl) complexes because stoichiometric methods often lead to ligand rearrangement.

Here, we report several new mono-Cp* lanthanide complexes binding a variety of ligands including Cl^{1-}, $(bipy)^{1-}$, $(bipy)^{2-}$, $(PhNNPh)^{2-}$, $(N_3)^{1-}$, and $(S_x)^{2-}$ (x = 4,5). In addition, these reactions have generated products in which $(bipy)^{1-}$ ligands are oriented parallel to each other with C···C distances which are shorter than the sum of the van der Waals radii of two carbon atoms, both inter- and intra-molecularly. Although the products described here were not synthetic targets for us, and hence optimized syntheses have not been pursued, they demonstrate that unusual structural types exist and can be accessed through the diverse reactivity of bipy-ligated lanthanide metallocene complexes.

Results and Discussion

A Mono-Cp* Nd Complex, $[K(crypt)]_2[Cp^*Nd(bipy)_2]$, 1

One of the attractive aspects of the $[Cp^*_2Ln(bipy)]^{1-}$ system outlined in Scheme 1 is that the $Cp^*_2LnCl(bipy)$ starting material can be prepared in a single reaction vessel from $LnCl_3$, 2 equiv. of KCp*, and one equiv. of bipy followed by two subsequent

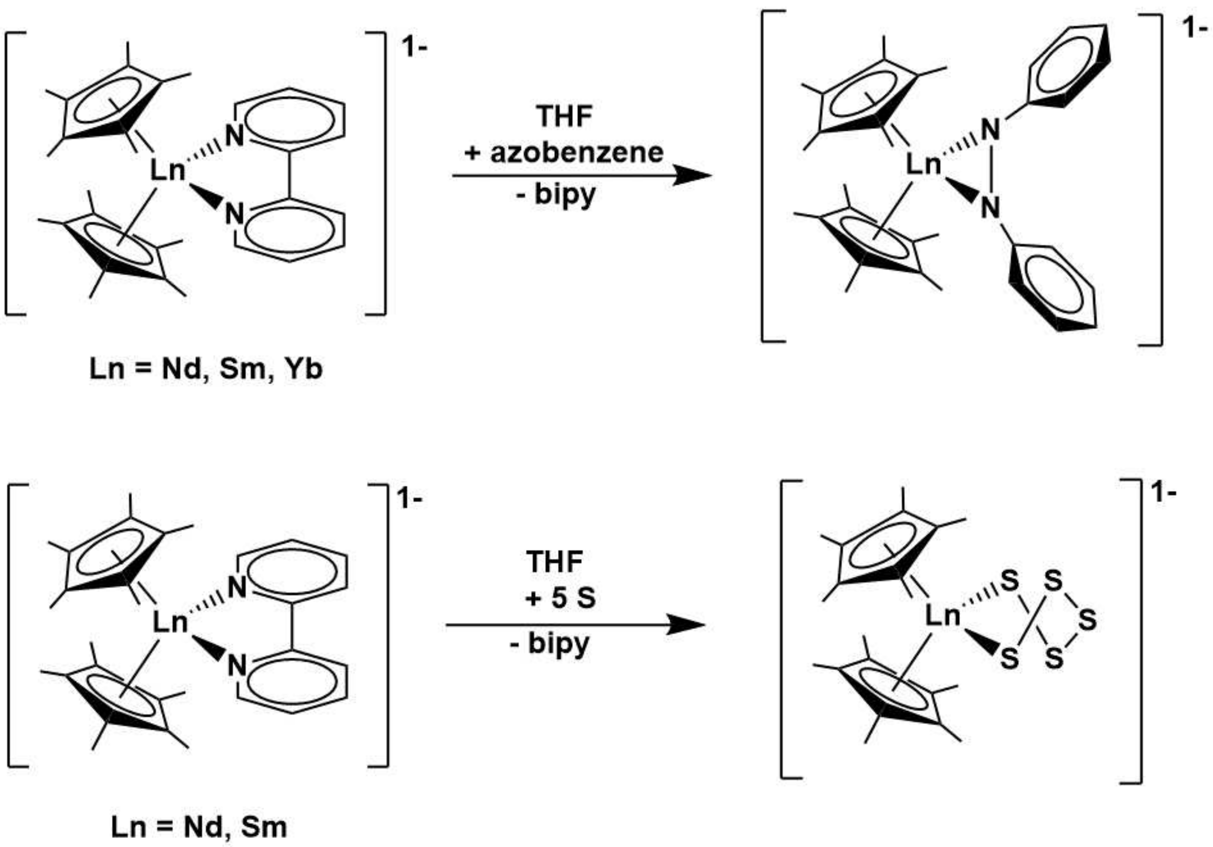

Scheme 2. Two electron reduction chemistry of $[Cp^*_2Ln(bipy)]^{1-}$

reductions to form the two-electron reductant. This is much more convenient than the synthesis of some other rare-earth multi-electron reducing agents involving Cp* ligands.[26–29] In an effort to further simplify the preparation of $[Cp^*_2Ln(bipy)]^{1-}$, we attempted to prepare $[Cp^*_2Nd(bipy)]^{1-}$ by combining the two reduction steps in Scheme 1 into a one-pot reaction of $Cp^*_2NdCl(bipy)$, 2.2.2-cryptand (crypt), and an excess of KC_8, reaction 1. However, although the desired $[K(crypt)][Cp^*_2Nd(bipy)]$ was indeed formed in this reaction, two new crystalline products were also isolated in low yield: the mono-Cp* complex, $[K(crypt)]_2[Cp^*Nd(bipy)_2]$, **1**, Figure 1, and the byproduct, $[K(crypt)][Cp^*_2NdCl_2]$, **2**, Figure 2.

Complex **1** is the first of a series of mono-Cp* complexes reported in this paper that arises from bipy metallocene reactions.

Complex **2** is a variant of the "ate" salts $Cp^*_2LnCl_2M(L_x)$,[30] commonly formed in reactions of two equiv. of KCp* with $LnCl_3$. Indeed, **2** was rationally synthesized through this route so that it could be characterized spectroscopically (see Experimental Section). However, structurally characterized bis-Cp* lanthanide complexes with two halide ligands typically have bridging halides, e.g. $Cp^*_2Ce(\mu\text{-}Cl)_2Li(OEt_2)_2$, $[Cp^*_2Ce(\mu\text{-}Cl)_2K(THF)]_n$,[31,32] $Cp^*_2Pr(\mu\text{-}Cl)_2Li(OEt_2)_2$,[30] $Cp^*_2Nd(\mu\text{-}Cl)_2Na(DME)_2$,[33] $[Cp^*_2Sm(\mu\text{-}Cl)_2K(THF)]_n$, $Cp^*_2Sm(\mu\text{-}Cl)_2Li(OEt_2)_2$,[34,35] $Cp^*_2Yb(\mu\text{-}Cl)_2Li(OEt_2)_2$, $Cp^*_2Yb(\mu\text{-}I)_2Li(OEt_2)_2$,[36] and $Cp^*_2Lu(\mu\text{-}Cl)_2Na(OEt_2)_2$.[37] In contrast to these examples, complex **2** has terminal chloride ligands due to the presence of the crypt chelate that binds the potassium. A similar result was previously found with the uranium complex $[K(crypt)][Cp^*_2UI_2]$.[38]

Selected metrical data on complexes **1** and **2** are compared with related complexes in Table 1.[23] A critical metric in the structural analysis of bipy complexes is the C_{bipy}–C'_{bipy} distance, which has been shown previously to be a useful indicator of the oxidation state of the bipyridine ligand (neutral, radical anionic, or dianionic). Thus, the C_{bipy}–C'_{bipy} distances of ca. 1.49 Å for $(bipy)^0$, 1.43 Å for $(bipy)^{1-}$, and 1.38 Å for $(bipy)^{2-}$ have been used as one indicator of the oxidation state of the bipy ligand.[39]

The 1.379(4) and 1.382(4) Å C_{bipy}–C'_{bipy} distances in **1** indicate the presence of two $(bipy)^{2-}$ dianions which indicates that this is a Nd(III) complex. This analysis is consistent with the presence of two $[K(crypt)]^{1+}$ countercations in its molecular structure. The complex has the structure of a four-legged piano stool. The Cp* ring centroid and the four nitrogen donor atoms comprise a distorted square pyramid with a τ^5 value of 0.20, where $\tau^5 = 0$ for a pure square pyramid and 1 for a pure trigonal bipyramid.[40]

Complex **2** has metrical parameters that are surprisingly similar to those of $Cp^*_2Nd(\mu\text{-}Cl)_2Na(DME)_2$,[33] which has bridging chloride ligands, Table 1. The 2.687(5) and 2.720(5)Å Nd–Cl distances in the latter complex are only slightly numerically longer than the 2.6779(9) Å in **2**. A similar situation was

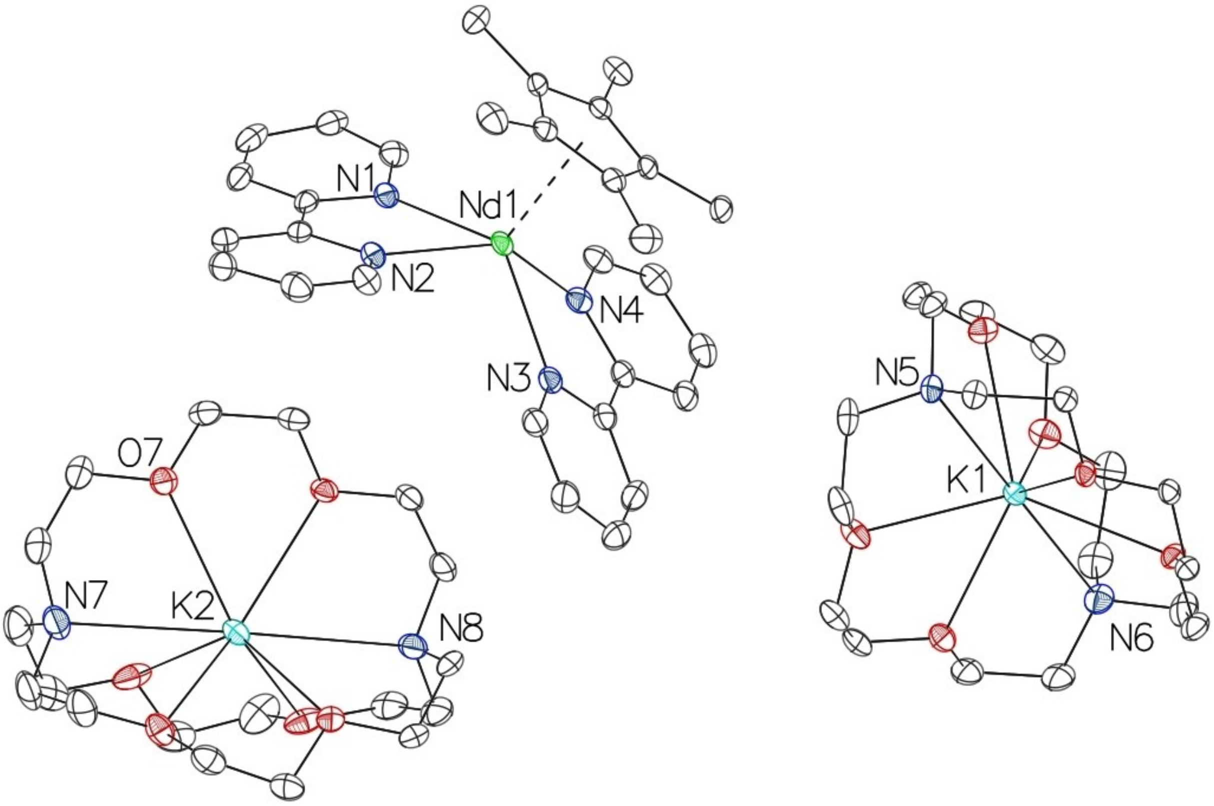

Figure 1. The molecular structure of $[K(crypt)]_2[Cp^*Nd(bipy)_2]$, **1**, with thermal ellipsoids drawn at 30 % probability. For clarity, hydrogen atoms, two solvent molecules of crystallization (THF), and modelled disorder at one cryptand are not shown.

Table 1. Selected bond distances (Å) and angles (°) in complexes **1** and **2** and additional Nd complexes featuring neutral and reduced bipy ligands.

	Ln–C (avg.)	Ln–Cp_{cent}	Ln–E (E=N or Cl)	C_{bipy}–C'_{bipy}	Cp_{cent}–Nd–Cp_{cemt}
$[Cp^*Nd(bipy)_2]^{2-}$ (**1**)	2.780(1)	2.507(1)	2.463(2), 2.427(2), 2.433(2), 2.467((2)	1.382(4), 1.379(4)	–
$Cp^*_2NdCl(bipy)$ [23]	2.7955(5)	2.5171(7), 2.5248(8)	2.6182(12), 2.7305(12)	1.485(2)	135.62(2)
$Cp^*_2Nd(bipy)$ [23]	2.7518(9)	2.4757(13), 2.4718(12)	2.463(2), 2.456(2)	1.427(4)	138.03(4)
$[Cp^*_2Nd(bipy)]^{1-}$ [23]	2.7901(6)	2.5077(8), 2.5260(9)	2.3876(16), 2.3940(16)	1.385(3)	134.96(3)
$[Cp^*_2NdCl_2]^{1-}$ (**2**)	2.766(1)	2.496(2)	2.6779(9)	–	136.87(8)
$(Cp^*_2Nd(\mu\text{–}Cl)_2Na(DME)_2$ [33]	2.76(2)	2.456(11), 2.518(10)	2.687(5), 2.720(5)	–	133.1(4)

observed with $[K(crypt)][Cp^*_2UI_2]$ and related complexes with bridging iodide ligands,[38] i.e. the metal-halide distances fall within a narrow range regardless of their terminal or bridging nature in these metallocene dihalides.

A Mono-Cp* Lu Complex: $Cp^*Lu(bipy)_2$, 3

Despite several attempts, we were unable to isolate $Cp^*_2LuCl(bipy)$ using the synthetic route described in Scheme 1. This difficulty is perhaps a result of the smaller size of Lu in comparison to the metals for which this route was successful. We therefore attempted to circumvent this problem with the intent of isolating a complex with a lower coordination number, e.g. $Cp^*_2Lu(bipy)$. However, in this case, the K/KI reduction of the reaction product of $LuCl_3$ with 2 equiv. of KCp* in the presence of bipy led to the mono-Cp* complex $Cp^*Lu(bipy)_2$, reaction 2, Figure 3.

The molecular structure of **3** displayed C_{bipy}–C'_{bipy} distances of 1.424(5) and 1.432(4) Å indicating that the bipy ligands are

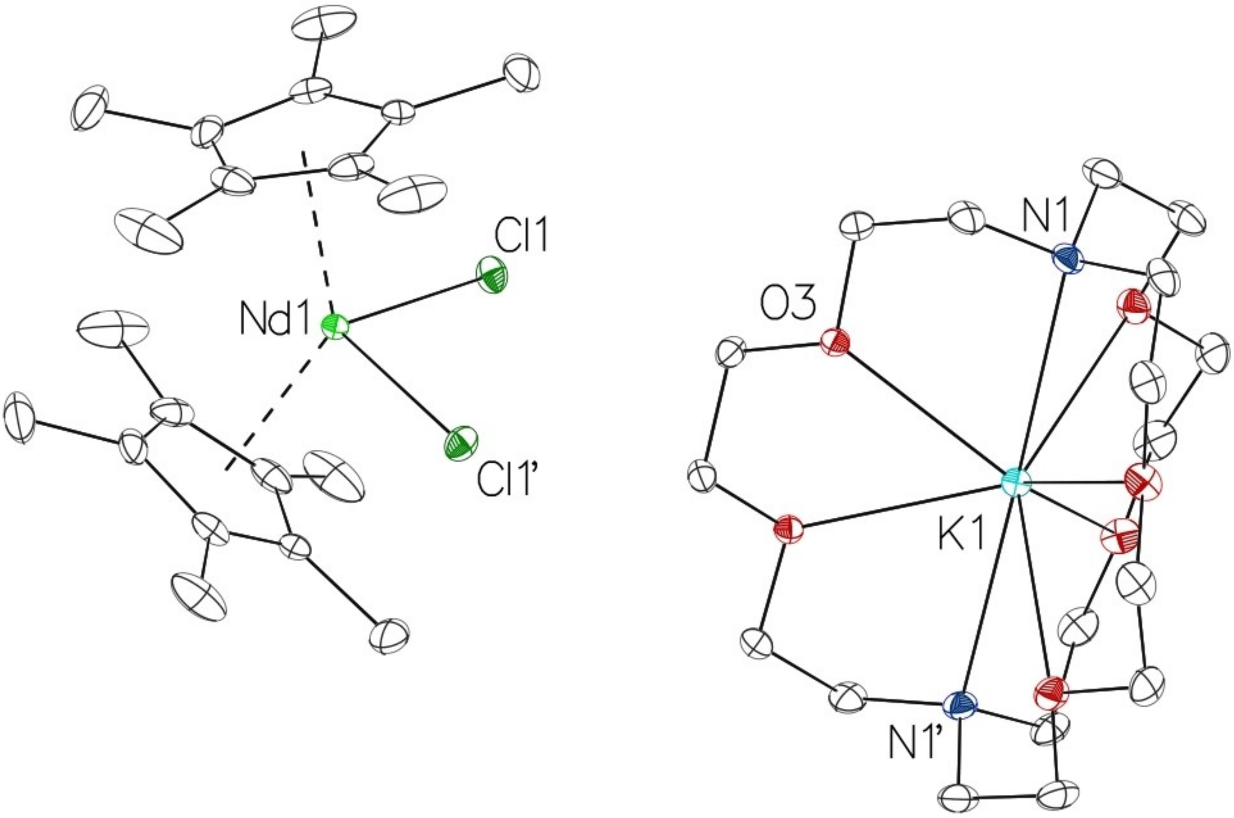

Figure 2. The molecular structure of [K(crypt)][Cp*$_2$NdCl$_2$], **2**, with thermal ellipsoids drawn at 30% probability. For clarity, hydrogen atoms and two solvent molecules of crystallization (THF) are not shown.

monoanionic and the compound contains a Lu(III) ion. Hence, complex **3** is a neutral Ln(III) analog of the dianionic Ln(III) complex, **1**. In support of the presence of (bipy)$^{1-}$ ligands, the EPR spectrum of complex **3** at 300 K displayed a signal with $g_x = 1.99$, $g_y = 2.01$, $g_z = 2.01$, Figure 4. This is consistent with the presence of a metal-bound radical bipy anion.[41–43] Although coupling to nitrogen is observed with $A_x = 57.7$ MHz (20.4 G), $A_y = 57.5$ MHz (20.5 G), and $A_z = 58.1$ MHz (20.6 G), no coupling to the ^{175}Lu nucleus (I = 7/2) was observed. While this observation agrees with the EPR spectrum of a recently reported Lu(III) complex binding a similar radical ligand which also showed no coupling to the ^{175}Lu nucleus,[44] it contrasts with other results that showed extensive coupling between the unpaired electron of the bipy radical anion and ^{135}La (I = 7/2) in the EPR spectrum of LaI$_2$(bipy)(bipy^{1-})(DME).[45]

Complex **3** exhibits unusual structural features in its crystal packing. As shown in Figure 5, there is proximity between (bipy)$^{1-}$ ligands of neighboring molecules in the crystal structure. The closest approach between carbon atoms of parallel (bipy)$^{1-}$ ligands is 3.289(4) Å, which is shorter than the sum of van der Waals radii of two carbon atoms, 3.4 Å.[46] These metrical parameters suggest that there is an attractive intermolecular interaction between bipy ligands of **3** in the solid state. This may explain in part its unusually high melting point (> 250 °C). Normally, attraction between two negatively charged ligands would be disfavored, but this may be ameliorated in this case by the highly Lewis acidic Lu(III) center. Similar attraction between the anionic bipy ligands have been observed in the Ln(bipy)$_4$ complexes of La and Ce, which feature close intermolecular C···C distances of 3.32 Å (La) and 3.24 Å (Ce).[47] As a result of these attractive interactions, these Ln(bipy)$_4$ complexes form polymeric chains in the solid state. In the case of complex **3**, the formation of such a polymer is less likely because the Lu atom is "capped" by the Cp* ligand.

If complex **3** is a closed-shell Lu(III) ion binding two radical anionic bipy ligands, it should have a total spin of S = 1. However, the room temperature solution magnetic moment (Evans' method) of **3** was measured to be 1.7 μ_B, which matches the value expected for a single unpaired electron (S = 1/2). Previously, for Lu(bipy)$_4$, a lower than expected magnetic moment, 1.88 μ_B, was also observed.[15] For this molecule, CASSCF calculations suggested that the lowest energy electronic states in Lu(bipy)$_4$ are multiconfigurational spin doublets (S = 1/2), rather than the S = 3/2 state expected if the complex contained three radical anionic bipy ligands and one neutral bipy ligand.[47] A similar situation could arise in **3** involving diamagnetic species such as Cp*Lu(bipy^{2-})(bipy^0) and antiferromagnetically coupled Cp*Lu(bipy^{1-})$_2$. In further support of this, the infrared spectrum of complex **3** displays two sharp absorbances at 722 and 680 cm^{1-}, which we previously noted

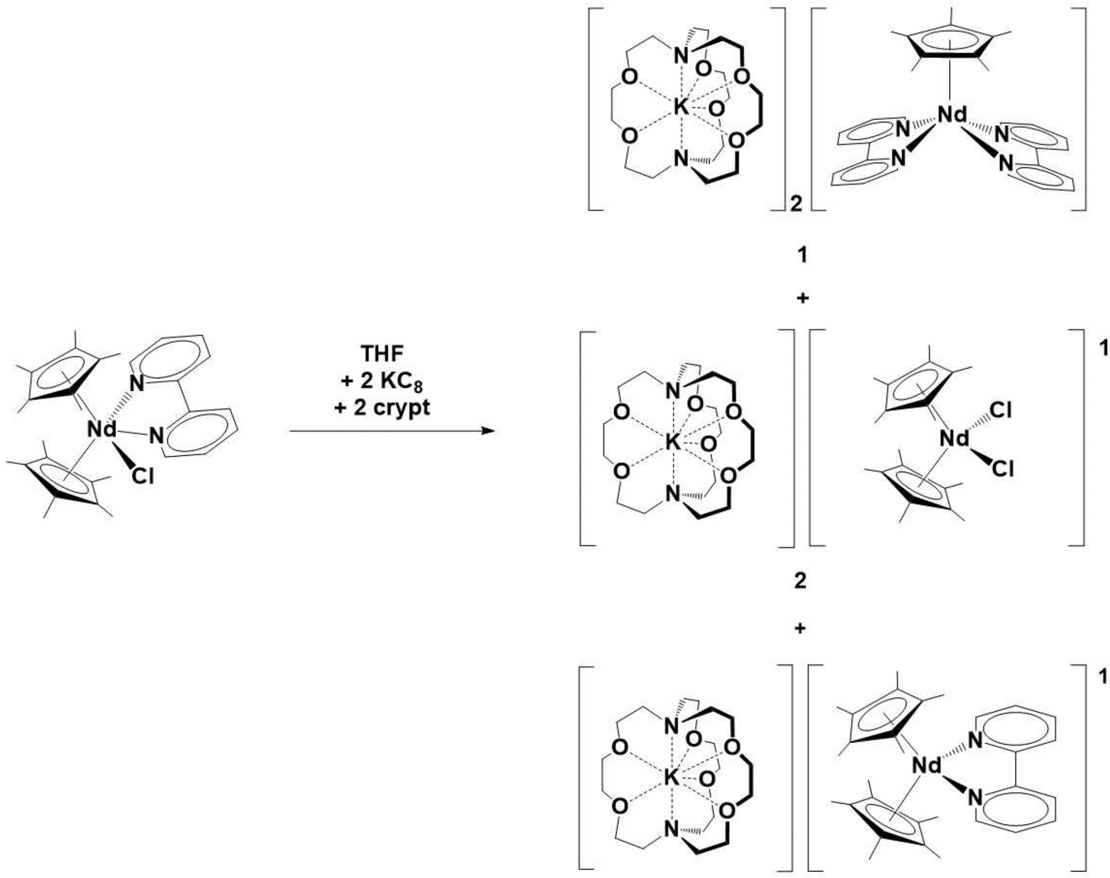

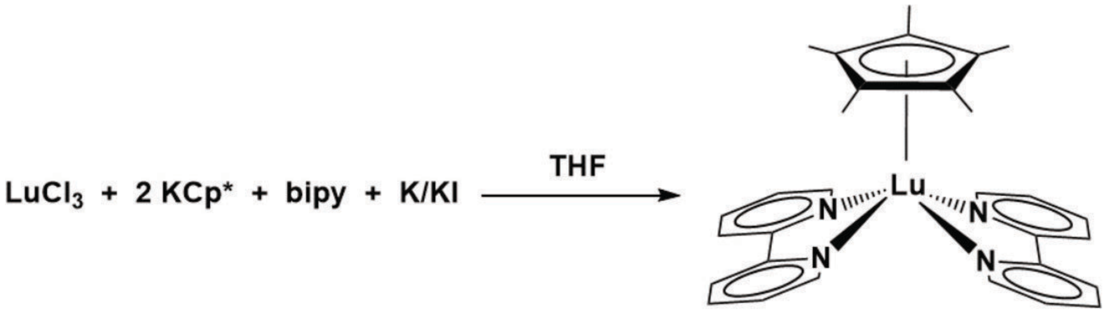

to be indicative of the presence of $(bipy)^{1-}$ and $(bipy)^{2-}$ ligands, respectively, in the $[Cp^*{}_2Ln(bipy)]^n$ series ($n = 0, -1$).[23] It is also worth noting that the dimeric nature of **3** may be at least partially preserved in solution.

Mono-Cp* Eu Complexes, $[K(crypt)]_2[Cp^*Eu(THF)(PhNNPh)]_2$, 4, and $[K(crypt)][Cp^*Eu(THF)(PhNNPh)]_2$, 5

A Eu complex with one Cp* ligand per metal was isolated by examination of the reaction chemistry of the Eu(II) $(bipy)^{1-}$ complex, $[K(crypt)][Cp^*{}_2Eu(bipy)]$, with azobenzene. This reaction had the potential to reduce PhN=NPh by two electrons to form a $[K(crypt)][Cp^*{}_2Eu^{III}(PhNNPh)]$ Eu(III) product in reactivity analogous to the Yb reaction in Scheme 1. However, the product isolated was a dimeric mono-Cp* Eu(II) complex, $[K(crypt)]_2[Cp^*Eu(THF)(PhNNPh)]_2$, **4**, reaction 3, Figure 6. The isolation of the Eu(II) product suggests that the reduction of the two equiv. of azobenzene was accomplished by the $(bipy)^{1-}$ and $(Cp^*)^{1-}$ ligands, although the reaction could be more complicated since it proceeded in low yield and no additional products containing Cp* were observed. $(Cp^*)^{1-}$ is known to be a reducing agent in sterically crowded complexes like the $Cp^*{}_3M$ rare-earth and actinide complexes,[26,48,49] but it also acts as a reductant in reactions like the synthesis of $Cp^*{}_2Eu(THF)$ from three equiv. of NaCp* and $EuCl_3$.[50]

In an attempt to prepare the $[K(crypt)][Cp^*{}_2Eu^{III}(PhNNPh)]$ target by reaction of $Cp^*{}_2Eu(THF)_2$ with $[K(crypt)][N_2Ph_2]$

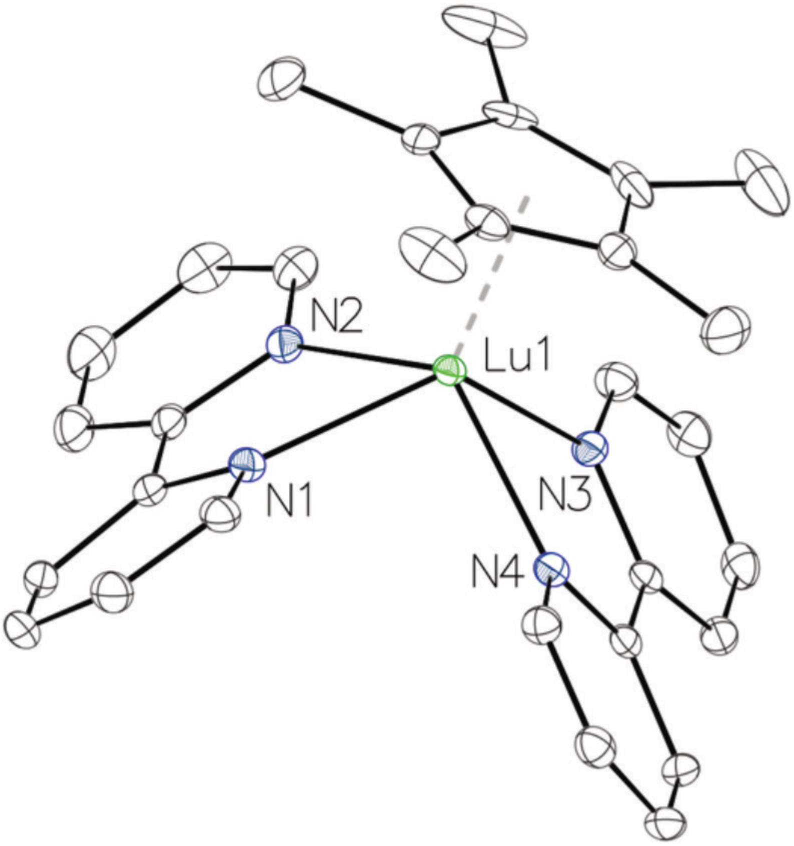

Figure 3. The molecular structure of Cp*Lu(bipy)$_2$, **3**, with thermal ellipsoids drawn at 30 % probability. For clarity, hydrogen atoms are not shown.

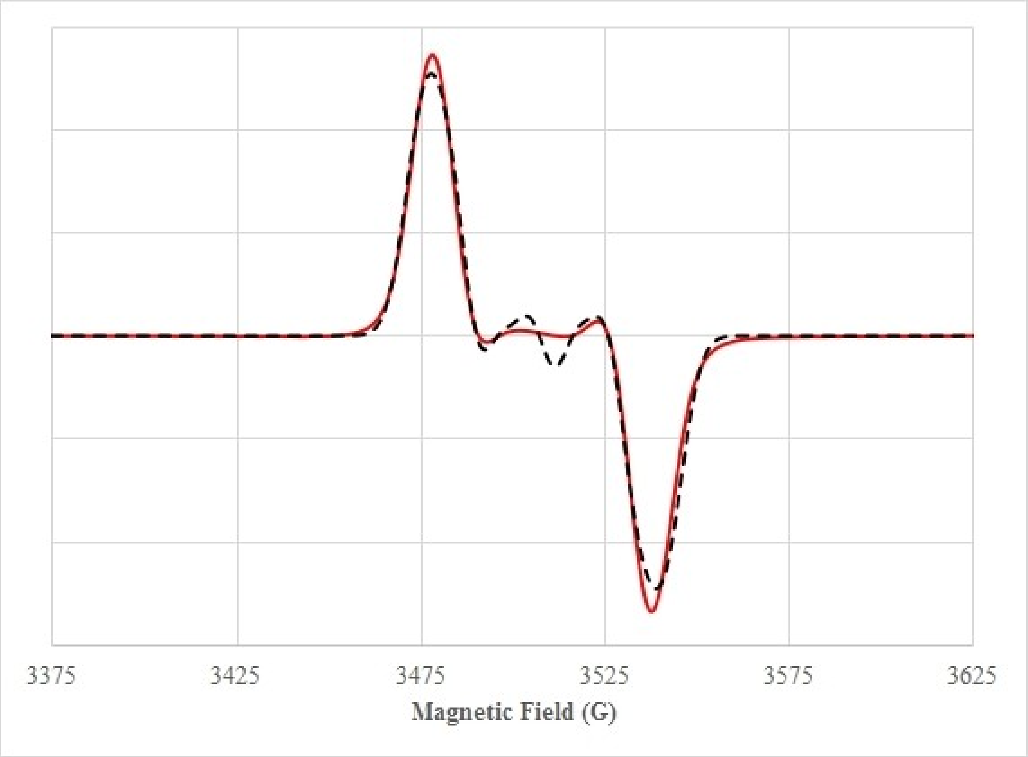

Figure 4. EPR spectra of Cp*Lu(bipy)$_2$ 300 K. The red trace is the experimental spectrum and the black dashed trace is the fitted spectrum.

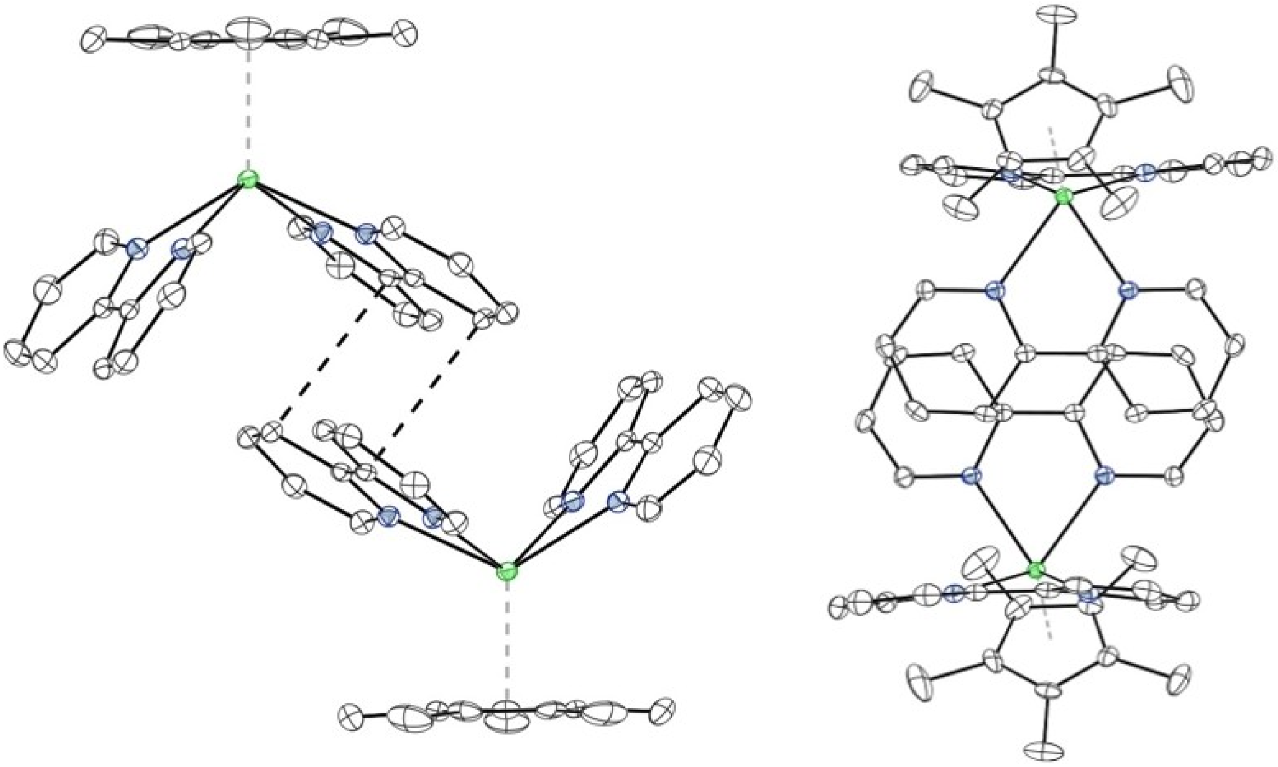

Figure 5. Two views of a pair of neighboring molecules of Cp*Lu(bipy)$_2$, **3**, with Lu shown in green and N shown in blue. The left image shows the two closest intermolecular approaches (3.289(4) Å) between carbon atoms of two bipy ligands, while the right image shows the displaced nature of the stacking of the bipy ligands in the crystal structure.

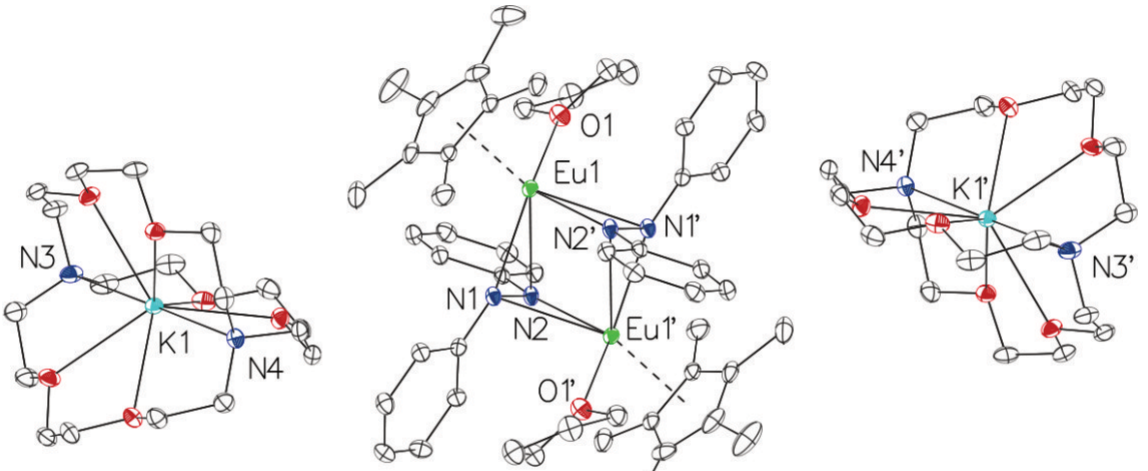

Figure 6. The molecular structure of [K(crypt)]$_2$[Cp*Eu(THF)(PhNNPh)]$_2$, **4**, with thermal ellipsoids drawn at 30 % probability. Selected structural metrics are shown in Table 2. For clarity, hydrogen atoms and solvent of crystallization (hexane, tetrahydrofuran) are not shown.

prepared *in situ*, another complex with one Cp* ligand per metal was obtained: the mixed-valent Eu^{II}/Eu^{III} complex [K(crypt)][Cp*Eu(THF)(PhNNPh)]$_2$, **5**, reaction 4, Figure 7. Isolation of these two analogous species allows a rare direct comparison of a Eu(II)/Eu(II) and Eu(III)/Eu(II) pair of compounds, Table 2.

Selected structural parameters of **4** and **5** are shown in Table 2 along with those of the neutral {Cp*Ln(THF)(PhNNPh)}$_2$ complexes of La[29] and Sm[51] for comparison. The dianionic Eu(II) dimer **4** possesses a crystallographically imposed inversion center located between the Eu atoms, and therefore the interatomic distances and angles around each Eu atom are identical. In contrast, every atom of the monoanionic Eu dimer, **5**, is crystallographically unique.

doi.org/10.1002/ejic.202300732

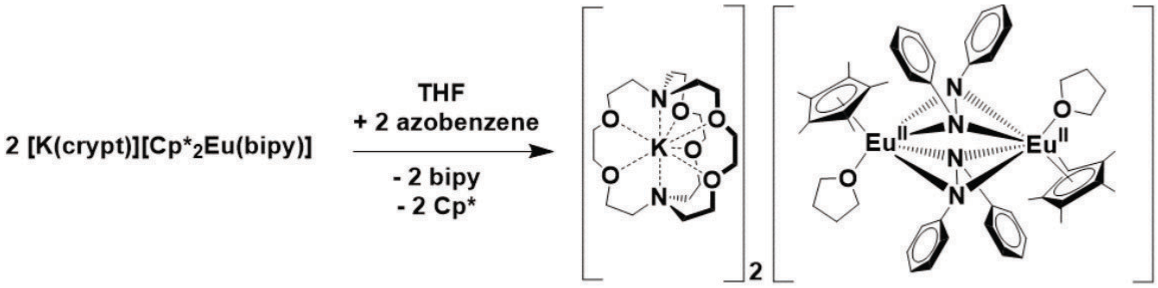

(3)

4

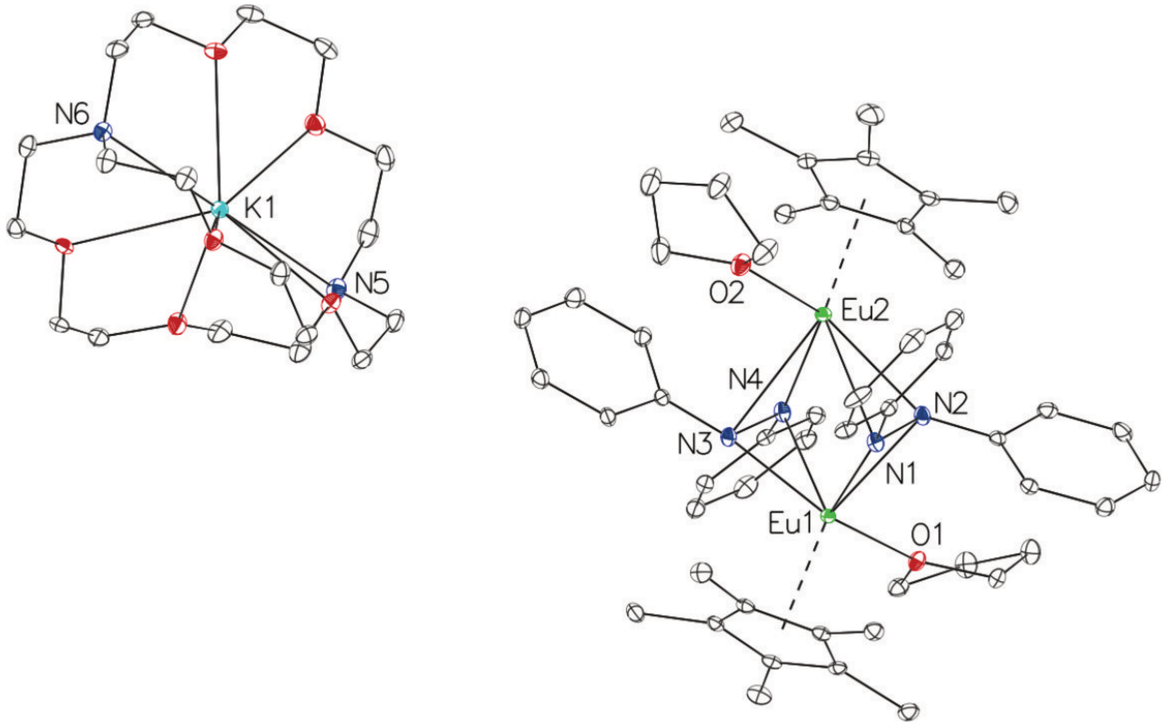

Figure 7. The molecular structure of [K(crypt)][Cp*Eu(THF)(PhNNPh)]$_2$, **5**, with thermal ellipsoids drawn at 30% probability. Selected structural metrics are shown in Table 2. For clarity, hydrogen atoms and solvent of crystallization (tetrahydrofuran) are not shown.

Table 2. Selected interatomic distances (Å) in complexes **4** and **5** and the related {Cp*Ln(THF)(PhNNPh)}$_2$ complexes of La and Sm.

	[Cp*Eu(THF)(PhNNPh)]$_2^{2-}$, **4**	[Cp*Eu(THF)(PhNNPh)]$_2^{1-}$, **5**	{Cp*La(THF)(PhNNPh)}$_2$[29]	{Cp*Sm(THF)(PhNNPh)}2[51]
N—N	N1—N2: 1.4652(1)	N1—N2: 1.468(5), N3—N4: 1.464(4)	N1—N2: 1.471(2)	N1—N1′: 1.44(1)
Ln—N	Eu1—N1: 2.730(2), Eu1—N2: 2.47(2), Eu1′—N1: 2.488(1), Eu1′—N2: 2.7525(2)	Eu1—N1: 2.292(3), Eu1—N2: 2.498(3), Eu1—N3: 2.289(3), Eu1—N4: 2.480(3), Eu2—N1: 2.849(3), Eu2—N2: 2.527(3), Eu2—N3: 2.815(3), Eu2—N4: 2.512(3)	La1—N1: 2.4202(16), La1—N2: 2.6346(16), La1—N1′: 2.6383(16), La—N2′: 2.4364(16)	Sm1—N1: 2.559(7), Sm1—N1′: 2.323(7)
Ln—Cnt	Eu1—Cnt1: 2.62(1)	Eu1—Cnt1: 2.48(1), Eu2—Cnt2: 2.59(1)	La1—Cnt1: 2.562	Sm1—Cnt1: 2.484
Ln—O	Eu1—O1: 2.6532(2)	Eu1—O1: 2.531(2), Eu2—O2: 2.640(2)	La1—O1: 2.6041(14)	Sm1—O1: 2.543(9)
Ln—Ln	Eu1—Eu1′: 3.6643(3)	Eu1—Eu2: 3.5698(2)	La1—La1′: 3.6408(7)	Sm—Sm1′: 3.491(2)

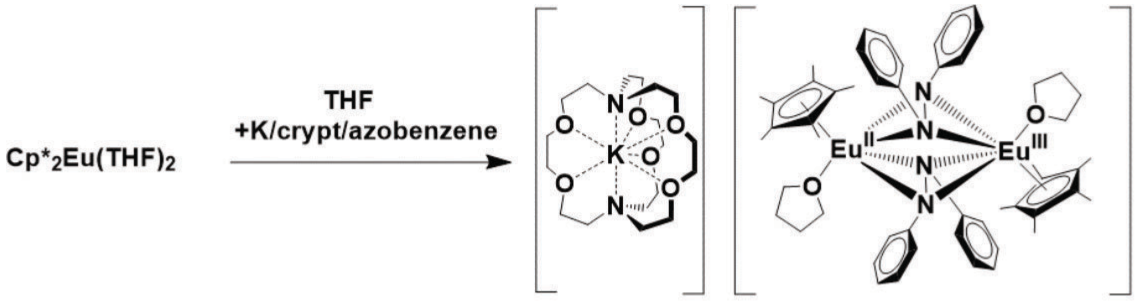

5

(4)

The N–N distances in the azobenzene components of **4** and **5** are similar to those of the $(PhNNPh)^{2-}$ dianions in the La and Sm complexes. All of the complexes in Table 2 have complementary pairs of Ln–N distances for each nitrogen donor atom, with one shorter distance on one side and a longer length on the other. Hence, the $(PhNNPh)^{2-}$ dianions are not located symmetrically between the metals.

Charge balance with the $(Cp^*)^{1-}$ and $[K(crypt)]^{1+}$ components gives the Eu(II)/Eu(II) and Eu(II)/Eu(III) oxidation state assignments for **4** and **5**, respectively. The 2.62(1) Å Eu–Cnt distance in **4** can be compared with the 2.57 Å and 2.55 Å distances in $Cp^*_2Eu(THF)_2$[24] and $\{Cp^*Eu(\mu\text{-}CCPh)\}_2)$,[25] which are also Eu(II) complexes. The Eu–Cnt distance in **4** also compares well with those in the La and Sm complexes when the differences in Shannon eight-coordinate radii are considered for Eu(II) (1.25 Å), La(III) (1.16 Å), and Sm(III) (1.079 Å).[52]

Complex **5** contains distinct sets of distances for each Eu atom. Thus, the 2.48(1) Å Eu1–Cnt1 and the 2.531(2) Å Eu1–O1 distances are each about 0.1 Å shorter than the 2.59(1) Å Eu2–Cnt2 and 2.640(2) Å Eu2–O2 distances. The latter Eu2 distances are similar to the corresponding Eu(II) distances in **4**. The shorter distances for Eu1 suggest it is Eu(III) since $4f^n$ Ln(III) complexes typically have bond distances 0.1–0.2 Å shorter than those of $4f^{n+1}$ Ln(II) complexes.[53] Hence, **5** appears to have distinct Eu^{II} (Eu2) and Eu^{III} (Eu1) ions which makes it a Robin-Day Class I mixed valence complex with trapped valences.[54]

Mono-Cp* Yb Complexes Through Reactions with Trimethylsilyl Azide and Elemental Sulfur. $[K(crypt)]_2[Cp^*Yb(N_3)_4]$, 6

The reactivity of the Yb(II) $(bipy)^{1-}$ complex, $[K(crypt)][Cp^*_2Yb(bipy)]$, with excess trimethylsilylazide, Me_3SiN_3, was examined to determine if $(Me_3SiN)^{2-}$ imido complexes could be accessed via two electron reductions facilitated by the reduced bipy complexes. Structurally authenticated lanthanide complexes featuring terminal imido ligands (RN^{2-}) are a rare class of molecules, the synthesis of which typically requires unusual methods.[55,56] Examples of such molecules are far more common for Th and U. Indeed, terminal imido complexes of these actinides have recently been shown to be accessible by the reaction of $Cp^{ttt}_2Th(bipy)$ and $Cp'''_2U(bipy)$ with organoazides (Cp^{ttt} = 1,3,4-tris(*tert*-butyl)cyclopentadienide, Cp''' = 1,3,4-tris(trimethylsilyl)cyclopentadienide).[17,19] Given the demonstrated ability of $Cp'''_2U(bipy)$ and $[Cp^*_2Ln(bipy)]^{1-}$ to function as 2 electron reductants, we sought to prepare terminal imido complexes by reaction of these $[Cp^*_2Ln(bipy)]^{1-}$ complexes with trimethylsilylazide.

However, instead of N–N cleavage, Si–N reductive cleavage occurred along with Cp*-loss to generate the mono-Cp* Yb(III) tetraazide complex, $[K(crypt)]_2[Cp^*Yb(N_3)_4]$, **6**, reaction 5, Figure 8. Since the formation of this tetra-azide product required at least 4 electrons for the Si–N cleavages, at least 2 equivalents of $[K(crypt)][Cp^*_2Yb(bipy)]$ must contribute to the formation of this product. Lanthanide polyazides have been synthesized in many different ways as reviewed in a recent article,[57] but to our knowledge only a single example of a lanthanide cyclopentadienyl complex binding a terminal azide ligand has been previously described, namely the anionic lutetium complex, $[K(crypt)]\{Cp^*Lu[MeC(N^iPr)_2](N_3)_2\}$.[58]

$[K(crypt)]_2[Cp^*Yb(N_3)_2(bipy)]$, 7a, and $[K(crypt)]_2[Cp^*Yb(N_3)_2(N_2C_{10}H_7SiMe_3)]$, 7b

To gain more control over the reaction that led to **6**, $[K(crypt)][Cp^*_2Yb(bipy)]$ was treated with 1 equiv. of Me_3SiN_3, reaction 6, rather than an excess. This again led to Si–N cleavage and generated another mono-Cp* complex, but in this case, it was an Yb(III) compound that retained a $(bipy)^{2-}$ ligand, $[K(crypt)]_2[Cp^*Yb(N_3)_2(bipy)]$, **7a**, Figure 9. The X-ray crystal structure of **7** contained another component in which a trimethylsilyl group had migrated to the bipy ligand, $[K(crypt)]_2[Cp^*Yb(N_3)_2(N_2C_{10}H_7SiMe_3)]$, **7b**. The X-ray data were modeled with a 2:1 ratio of **7a**:**7b**. Clearly, this reaction chemistry is complicated because the $(bipy)^{1-}$ ligand, which was one of the reducing components of the starting material, was not only retained in complex **7**, but it was further reduced by one electron to $(bipy)^{2-}$. The reaction is further complicated by the trimethylsilyl substitution byproduct. Alkylation of bipyridine is known through its reaction with alkyllithium reagents[59] and silylation of bipyridyl carbons is possible through a variety of means.[60–62] However, the silylation of bipyridine by its reaction with trimethylsilylazide is highly unusual and highlights the difficulty of predicting the outcome of these reactions, even when the stoichiometry is carefully controlled.

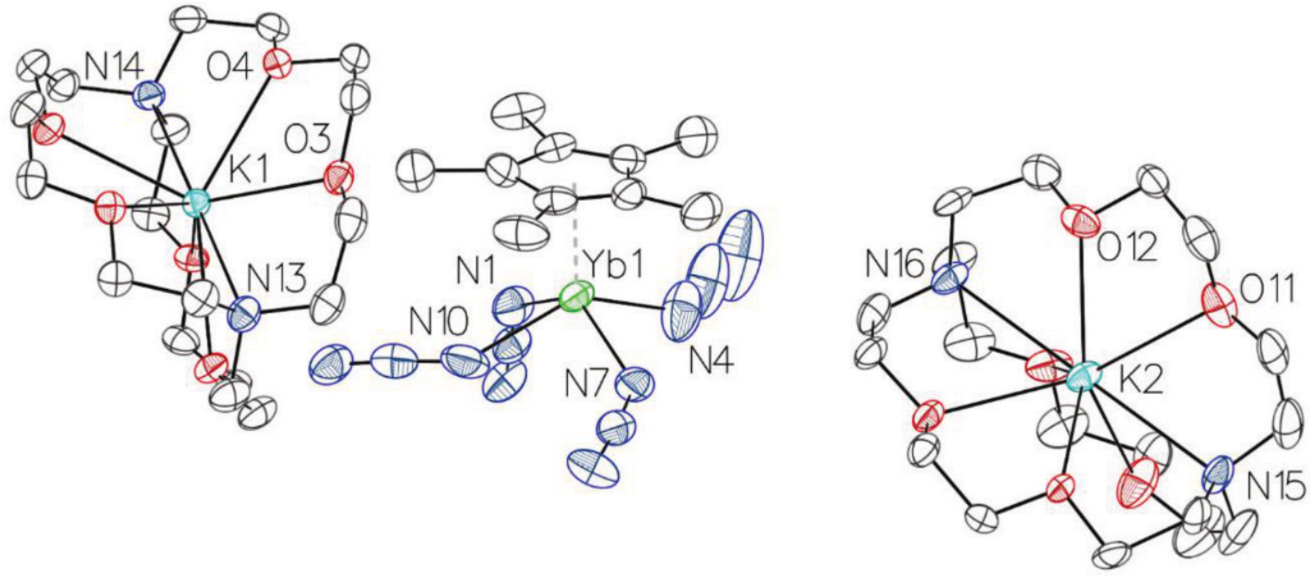

Figure 8. The molecular structure of [K(crypt)]$_2$[Cp*Yb(N$_3$)$_4$], **6**, with thermal ellipsoids drawn at 30 % probability. For clarity, hydrogen atoms and modelled positional disorder at multiple sites are not shown.

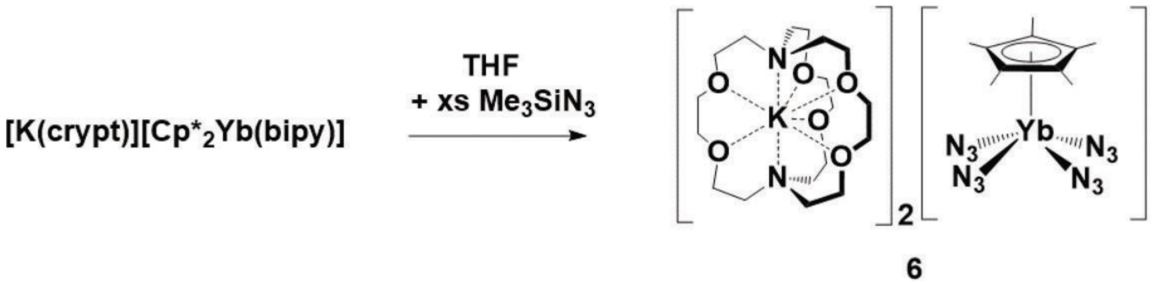

(5)

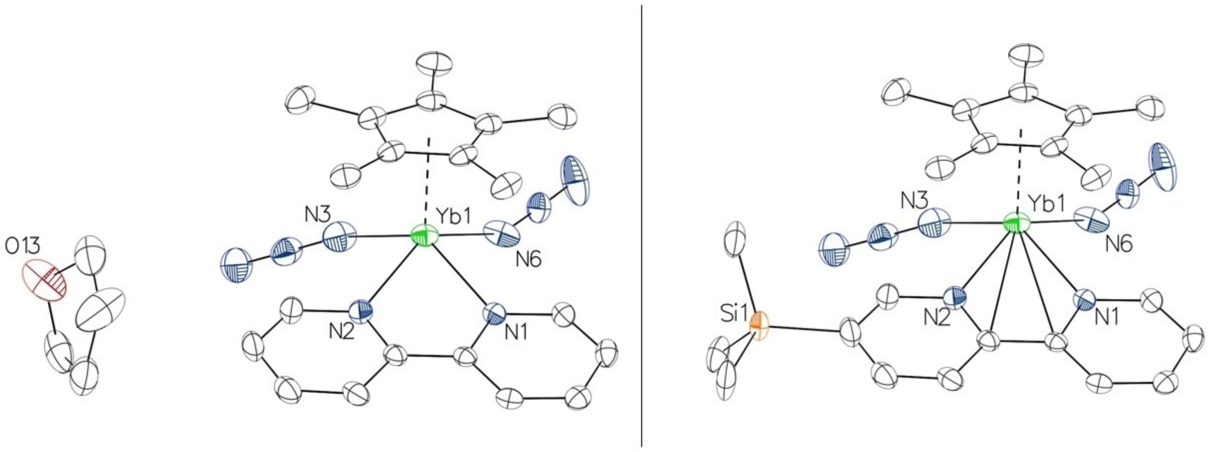

Figure 9. Molecular structures of the anions in product **7**: major (left) [K(crypt)]$_2$[Cp*Yb(N$_3$)$_2$(bipy)], **7 a**, and minor (right) [K(crypt)]$_2$[Cp*Yb-(N$_3$)$_2$(N$_2$C$_{10}$H$_7$SiMe$_3$)],**7 b**, with thermal ellipsoids drawn at 30 % probability. For clarity, hydrogen atoms are not shown.

Complexes **6** and **7** have four-legged piano stool structures like those of **1** and **3**. These four complexes provide a nice series of mono-Cp* complexes with two chelating bipy ligands (**1**, **3**), one chelating bipy ligand (**7 a**), and a complex with four nitrogen donor atoms that are not chelating (**6**). Selected metrical parameters of these complexes are compared in Table 3. The ring centroids and the four nitrogen donor atoms again define square pyramids with low 0.01- 0.05 $\boldsymbol{\tau}^5$ values indicative of nearly ideal square pyramidal geometry in all cases.

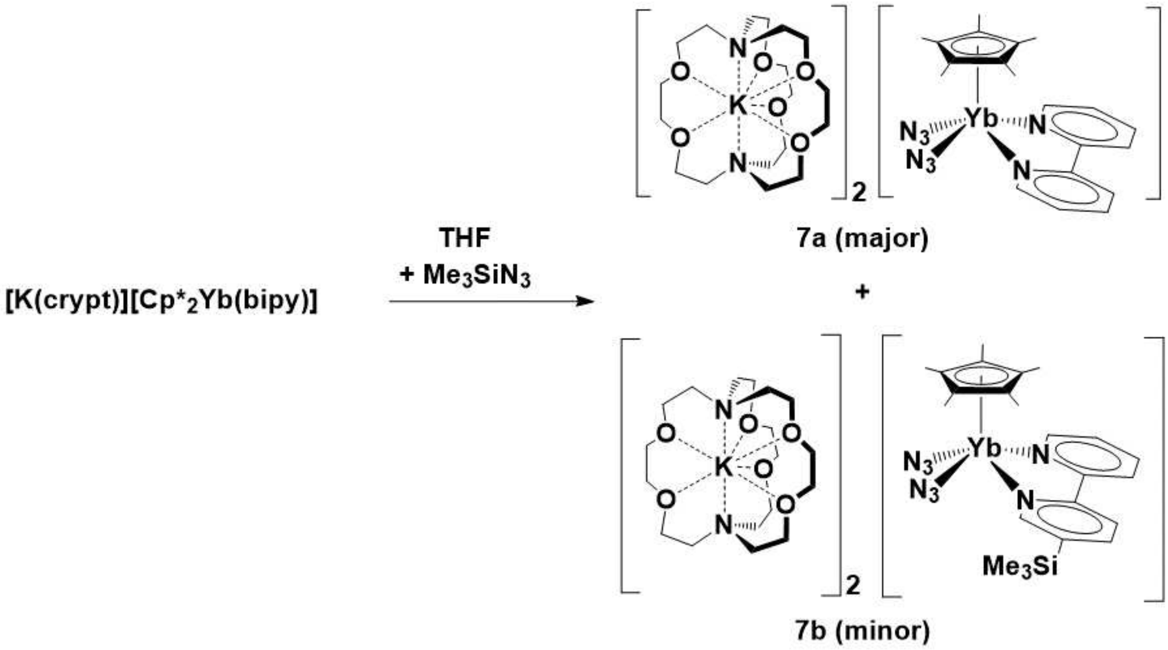

(6)

Table 3. Selected interatomic distances (Å) and angles (°) in piano stool complexes **1**, **3**, **6**, and **7**.						
	Ln–Cnt	**Ln–N**	**C_{bipy}–C'_{bipy}**	**Cnt–Ln–N**	**N–Ln–N**	**τ^5**
$[Cp^*Nd(bipy)_2]^{2-}$, 1	2.507(1)	2.426(2) 2.463(2) 2.433(3) 2.467(2)	1.383(4) 1.379(4)	114.40(6) 111.33(6) 105.94(6) 114.74(6)	66.43(8) 66.98(8) 97.19(8) 97.69(8) 130.82(7) 142.73(7)	0.20
$Cp^*Lu(bipy)_2$, 3	2.30(1)	2.323(3) 2.330(3) 2.314(3) 2.302(3)	1.423(5) 1.431(4)	119.04(8) 120.07(8) 113.37(8) 112.74(7)	69.69(9) 70.23(9) 86.86(9) 87.06(9) 127.15(9) 127.52(9)	0.01
$[Cp^*Yb(N_3)_4]^{2-}$, 6[a]	2.33(2)	2.02(1)–2.55(1) avg: 2.30(1)	–	100.0(5)–116.7(7) avg: 110.6(5)	48.6(8)–143.2(4) avg: 80.3(8)	0.01
$[Cp^*Yb(N_3)_2(bipy)]^{2-}$, 7[b]	2.33(1)	2.274(2) 2.282(3) 2.272(4) 2.297(4)	1.377(4)	112.00(7) 111.05(7) 110.74(9) 108.34(10)	70.15(9) 86.51(13) 88.34(12) 86.42(9) 136.38(11) 139.48(10)	0.05

[a] The structure of complex **6** is highly disordered and the table values are thus given as averages. [b] A single set of metrical parameters was observable for the **7a**/**7b** disordered structure.

$[K(crypt)]_2[Cp^*Yb(S_4)(S_5)]$, 8a, and $[K(crypt)]_2[Cp^*Yb(S_4)_2]$, 8b

As described in Scheme 2, the treatment of $[K(crypt)][Cp^*_2Ln(bipy)]$ (Ln=Nd, Sm) with elemental sulfur resulted in the reduction of sulfur by two electrons and the formation of Ln(III) complexes binding an $(S_5)^{2-}$ ligand. In an effort to extend this chemistry to the later lanthanide elements, the Yb(II) $(bipy)^{1-}$ complex, $[K(crypt)][Cp^*_2Yb(bipy)]$, was treated with elemental sulfur under the same conditions, reaction 7.

However, unlike the reactions with Nd and Sm in Scheme 2, the analogous reaction between the Yb complex and sulfur afforded a mono-Cp* system which is substitutionally disordered such that there are two Yb species in the crystal structure: $[Cp^*Yb(S_4)(S_5)]^{2-}$, **8a**, Figure 10, and $[Cp^*Yb(S_4)_2]^{2-}$, **8b**, reaction 7. The nature of this disorder is shown in Figure 11. Charge balance between $(Cp^*)^{1-}$, two $(S_n)^{2-}$ ligands, and two K(crypt) countercations, indicates that **8** is a complex of Yb(III).

We had previously found several cases wherein $[Cp^*_2Ln(bipy)]^{1-}$ is a competent two-electron reductant, including in the reaction between $[Cp^*_2Yb(bipy)]^{1-}$ and azobenzene in Scheme 2. However, the reduction of sulfur by $[Cp^*_2Yb(bipy)]^{1-}$ to form **8** is formally a four-electron process. Multiple equiv-

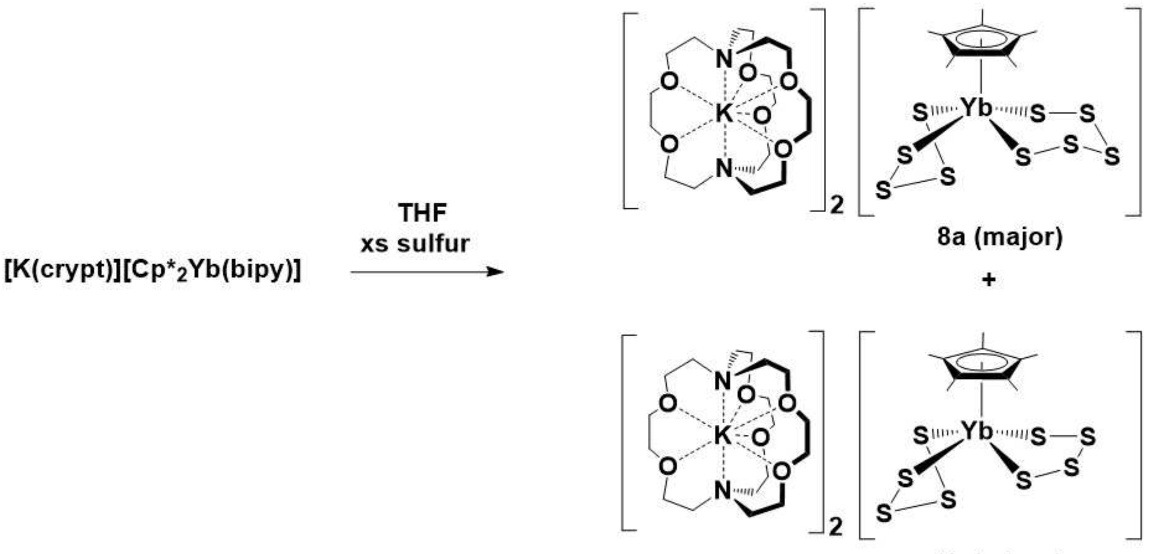

8a (major)

+

8b (minor)

(7)

alents of $[Cp^*_2Yb(bipy)]^{1-}$ may be involved in the reaction as well as $(Cp^*)^{1-}$ ligands as described above.

While cyclic MS_4 tetrathiametallolanes are known for transition and main group elements, e.g., Cp_2MoS_4 and (Ar)(Ar′)MS_4 (Ar = 2,4,6-trimethylphenyl; Ar′ = 2,4,6-bis(trimethylsilyl)methylphenyl; M=Si, Ge, Sn), the rare-earth structures most similar to **8a** and **8b** are the trimetallic complexes $[(DippForm)_3Ln_3S_{12}]$ (DippForm = *N,N′*-bis(2,6-diisopropylphenyl)formamidinate); Ln=Sm, Yb), which contain bridging, μ-η^3-S_4^{2-} ligands.[63] Although MS_5 complexes are known for both rare-earth and actinide metals, complexes **8a** and **8b** are apparently the only examples of such a simple MS_4 unit involving an *f* block element. Although the mixed polysulfide nature of **8** is unusual, "$M(S_x)(S_y)$" complexes have been reported elsewhere as exemplified by $Cp^*Re(S_3)(S_4)$[64] and $[PPh_4][In(S_4)(S_6)Cl]$.[65]

Further Reduction of $Cp^*_2Ln(bipy)$ Complexes. $[K(18\text{-c-}6)(THF)][Yb(bipy)_4]$, 9

Attempts to reduce $Cp^*_2Yb(bipy)$ further with 1 equiv. of KC_8 in the presence of 18-crown-6 in tetrahydrofuran, generated dark violet crystals of $[K(18\text{-c-}6)(THF)][Yb(bipy)_4]$, **9**, reaction 8, Figure 12. In contrast to the many mono-Cp* forming reactions above, in this reaction both Cp* ligands of the starting material were lost.

Complex **9** is an anionic analogue of the neutral $Ln(bipy)_4$ complexes that had been previously prepared by Herzog and coworkers nearly 60 years ago.[12,13] Subsequently, the $[Li(THF)_4][Ln(bipy)_4]$ complexes (Ln=Tb, Dy) were reported by Andersen and coworkers in a comprehensive study that details the multi-configurational nature of the bonding in the anions and the neutral species. A preparative route was also described wherein the reduction of Cp''_3Ln ($Cp''=C_5H_3(SiMe_3)_2$-1,3) with lithium metal in the presence of 2,2′-bipyridine afforded $Ln(bipy)_4$ or $[Ln(bipy)_4]^{1-}$.[47] Thus, while the isolation of complex **9** through the route described in reaction 8 is somewhat surprising given our previous success in isolating $[Cp^*_2Ln(bipy)]^{1-}$ complexes using crypt as a chelate, there is precedent

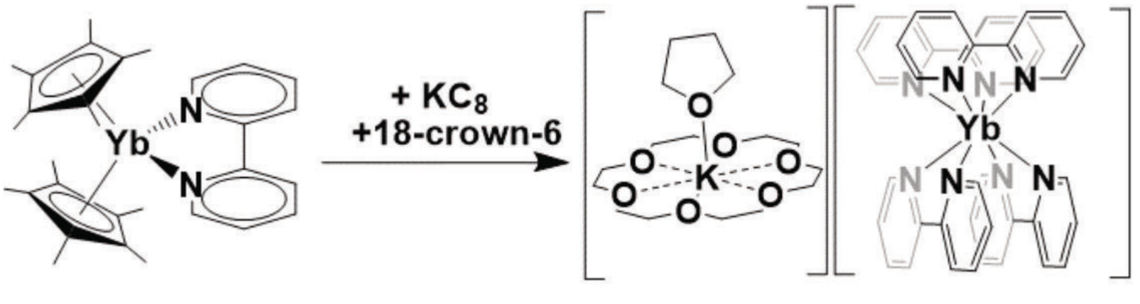

9

(8)

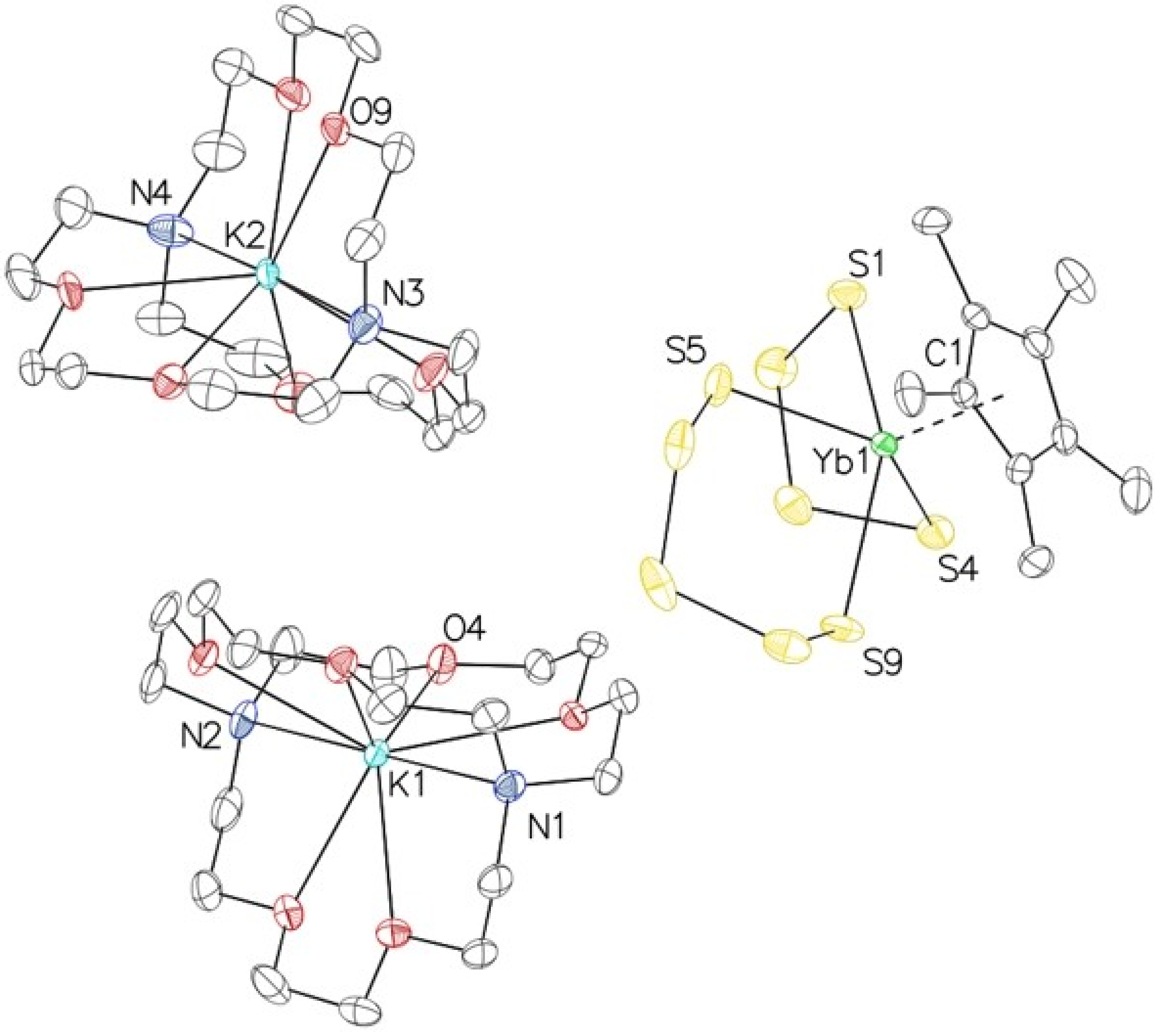

Figure 10. The molecular structure of the major (60 %) component of $[K(crypt)]_2[Cp^*Yb(S_4)(S_5)]$, **8a**, with thermal ellipsoids drawn at 30 % probability. For clarity, hydrogen atoms, substitutional disorder of the S_5/S_4 ligand involving the S5–S9 ring (vide infra), and modeled disorder involving one cryptand are not shown.

for the formation of this class of complexes through elimination of cyclopentadienyl ligands.

Selected distances and angles of **9** and its neutral analogue $Yb(bipy)_4$ are shown in Table 4. There is no crystallographically imposed symmetry within the $[Yb(bipy)_4]^{1-}$ anion of **9**, so each of these distances is unique. The C_{bipy}–C'_{bipy} distances in the bipy ligands of **9** are identical within experimental error at 1.43 Å and the Yb–N distances are within a narrow range of 2.414(3) to 2.455(3) Å. This is consistent with the presence of $(bipy)^{1-}$ monoanions and an assignment of Yb(III) binding four

Table 4. Selected interatomic distances (Å) and angles (°) of $[Yb(bipy)_4]^{0/1-}$ complexes.[a]

	C_{bipy}–C'_{bipy}	Ln–N	Ln–N–Cnt	
$Yb(bipy)_4$ [15]	1.477(11)	{2.516(6), 2.559(6)}	{175.87(14), 176.07(13)}	Square Antiprism
	1.386(13)	{2.440(8), 2.403(6)}	{179.08(17), 179.32(16)}	
	1.420(11)	{2.435(6), 2.416(6)}	{178.77(13), 178.01(15)}	
	1.420(11)	{2.423(6), 2.423(6)}	{178.21(16), 179.57(14)}	
$[Yb(bipy)_4]^{1-}$, **9**	1.427(7)	{2.429(3), 2.455(3)}	{172.00(7), 172.48(7)}	Cubic
	1.429(7)	{2.429(3), 2.414(3)}	{172.52(8), 171.49(8)}	
	1.425(7)	{2.435(3), 2.431(3)}	{172.47(7), 171.99(7)}	
	1.425(7)	{2.429(3), 2.430(3)}	{172.92(8), 173.15(7)}	

[a] Note: values in each horizontal row correspond to the same bipy ligand.

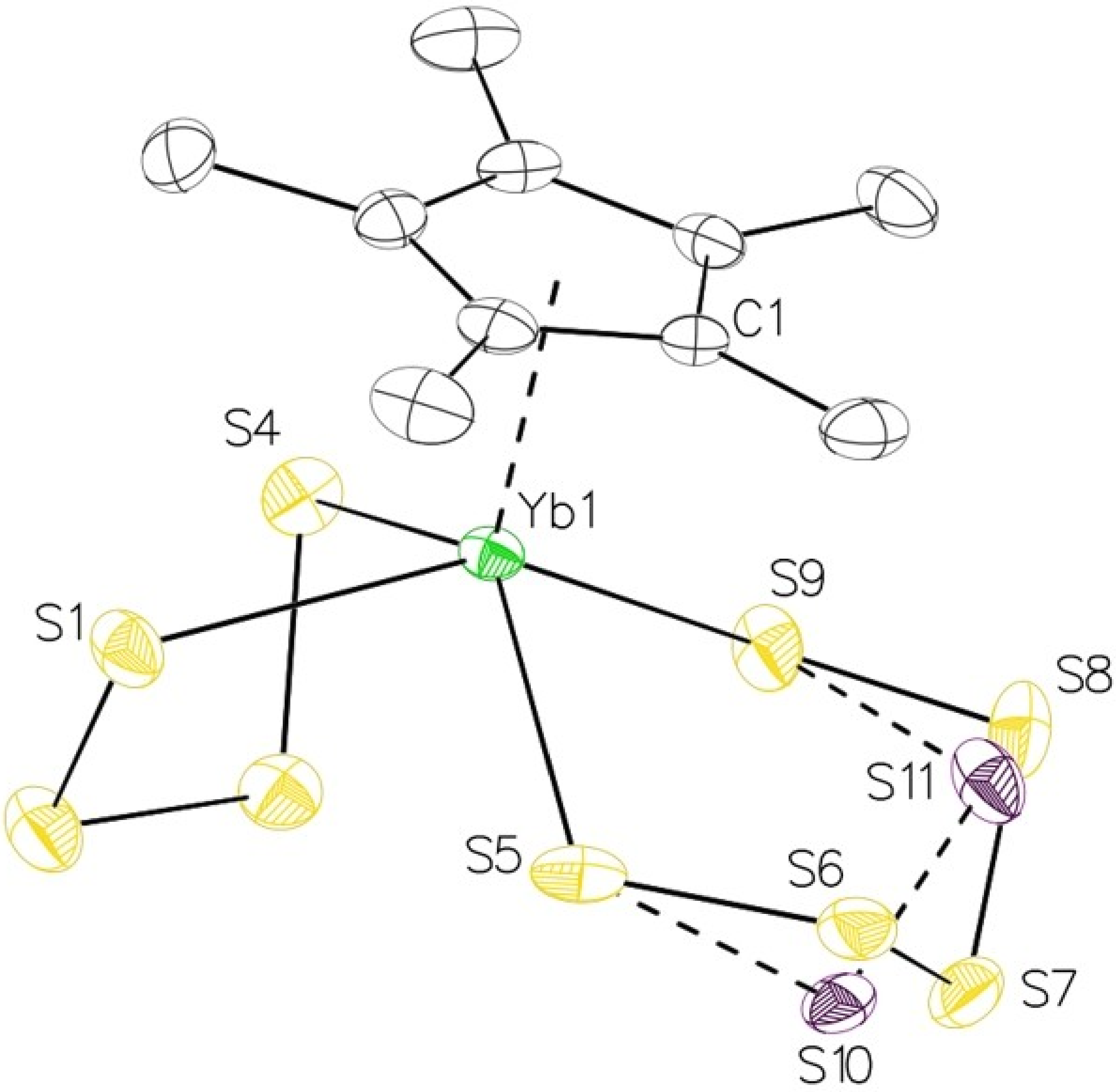

Figure 11. The molecular structure of the anion $[Cp^*Yb(S_4)(S_{5/4})]^{2-}$ in **8** showing the substitutional disorder at one sulfur ligand with the major (60 %) component drawn in yellow and the minor (40 %) component drawn in violet.

$(bipy)^{1-}$ ligands. In contrast, $Yb(bipy)_4$ has been evaluated as an Yb(III) complex with three $(bipy)^{1-}$ ligands and one neutral bipy ligand. In that complex, the C_{bipy}–C'_{bipy} distances range from 1.386(13) to 1.477(11) Å and Yb–N distances range from 2.403(6) to 2.559(6) Å.

As shown in Figure 13, the 8 nitrogen atoms in **9** comprise a slightly distorted cubic coordination geometry around the Yb atom. The N–N–N angles at each of the nitrogen apices range from 87.904(2)° to 92.089(2)°. The four N–N–N angles associated with each of the six faces sum to ca. 360° to give the cubic structure. A close examination of the structure of **9** reveals one substantial difference between its structure and those of the other known $[Ln(bipy)_4]^{1-}$ complexes. As shown in Figure 13, the two pairs of adjacent bipy ligands in **9** are significantly bent toward each other. As such, the Yb–N-(NC_5 centroid) angles in this complex range from 156.749(3)° to 161.189(1)° in comparison to the corresponding angles found in the other $[Ln(bipy)_4]^{0/1-}$ complexes, which are nearly linear in all cases. All of the nitrogen atoms in anionic **9** thus display pyramidal geometry.

There are several close interligand C···C approaches in **9** ranging from 2.967(7) to 3.199(6) Å which are shorter than the sum of their van der Waals radii, 3.4 Å.[46] The furthest approach between two corresponding carbon atoms of facing bipy ligands is ca. 4.05 Å. Additionally, each nitrogen atom of a bipy ligand is close to another nitrogen in another bipy ligand. The following pairs, N1 and N4, N2 and N3, N6 and N7, and N5 and N8, have 2.696(5) to 2.778(5) Å interligand N···N contacts which

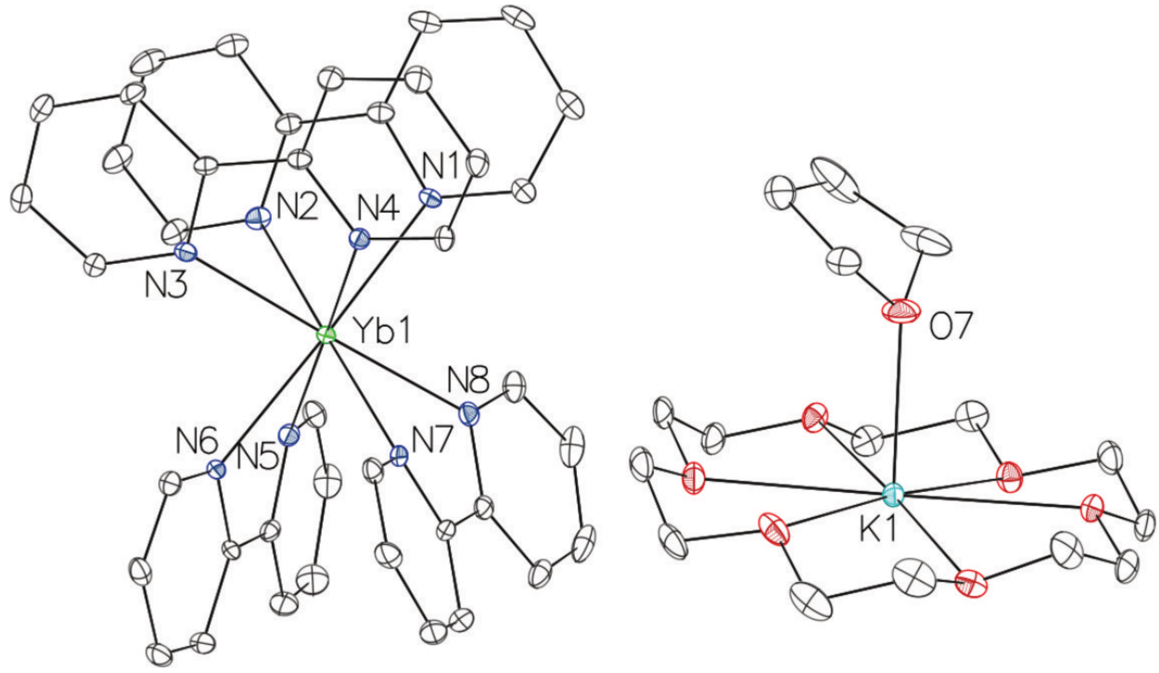

Figure 12. The molecular structure of [K(18-c-6)(THF)][Yb(bipy)$_4$], **9**, with thermal ellipsoids drawn at 30% probability. For clarity, hydrogen atoms are not shown.

are again shorter than the 3.1 Å sum of their van der Waals radii.[46] This suggests that there is a substantial attractive interaction between neighboring bipy ligands, although the nature of this interaction remains unclear in the absence of additional data. A similar distortion is also present in the actinide species U(bipy)$_4$ and [U(bipy)$_4$]$^{1-}$, wherein one pair of bipy ligands in each of the complexes displays this distortion.[66]

A Cp* Inverse Sandwich Salt [K$_2$(18-c-6)$_2$Cp*]$_2$[Cp*$_2$Sm(bipy)]$_2$·K(18-c-6)Cp*, 10

Since previous attempts to further reduce the Sm(III) (bipy)$^{2-}$ complex, [K(crypt)][Cp*$_2$Sm(bipy)], with K/crypt afforded no crystalline material,[23] we examined the reduction chemistry of Cp*$_2$Sm(bipy) with K and 18-crown-6 (18-c-6) as the chelate. When Cp*$_2$Sm(bipy) was treated with 2 equiv. of KC$_8$ and an excess of 18-crown-6, the salt, [K$_2$(18-c-6)$_2$Cp*]$_2$[Cp*$_2$Sm(bipy)]$_2$[K(18-c-6)Cp*], **9**, was isolated as brown crystals in low yield, reaction 9, Figure 14.

The structure of **10** contains two unique [Cp*$_2$Sm(bipy)]$^{1-}$ units. Although positional disorder is present in one of the bipy ligands in this structure, the average C$_{bipy}$–C′$_{bipy}$ distance in complex is 1.353(8) Å and the average Sm–N distance is 2.358(6) Å. These values are similar to those previously reported for [K(crypt)][Cp*$_2$Sm(bipy)] (C$_{bipy}$–C′$_{bipy}$: 1.383(3) Å; Sm–N: 2.3568(19), 2.3600(16) Å) and therefore are consistent with a Sm^{III}/(bipy^{2-}) formulation for **10**.[23] Thus, while the structure of the anion of **10** is essentially the same as the previously reported [Cp*$_2$Sm(bipy)]$^{1-}$ anion, the presence of [K$_2$(18-c-6)$_2$Cp*]$^+$ cations and the neutral K(18-c-6)Cp* unit in its structure indicate that other samarium-containing products with less than two Cp* ligands per metal are probably formed in this reaction. This is consistent with the formation of the several mono-Cp* complexes described earlier. Furthermore, the presence of the [K$_2$(18-c-6)$_2$Cp*]$^+$ cations in the structure of **10** highlights the importance of selecting an appropriate

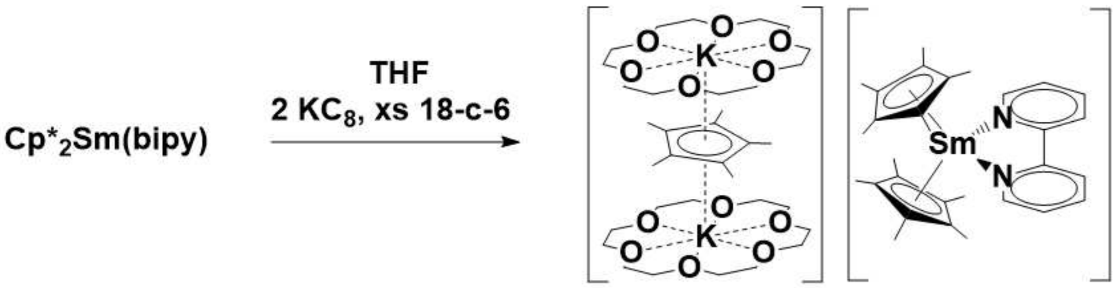

(9)

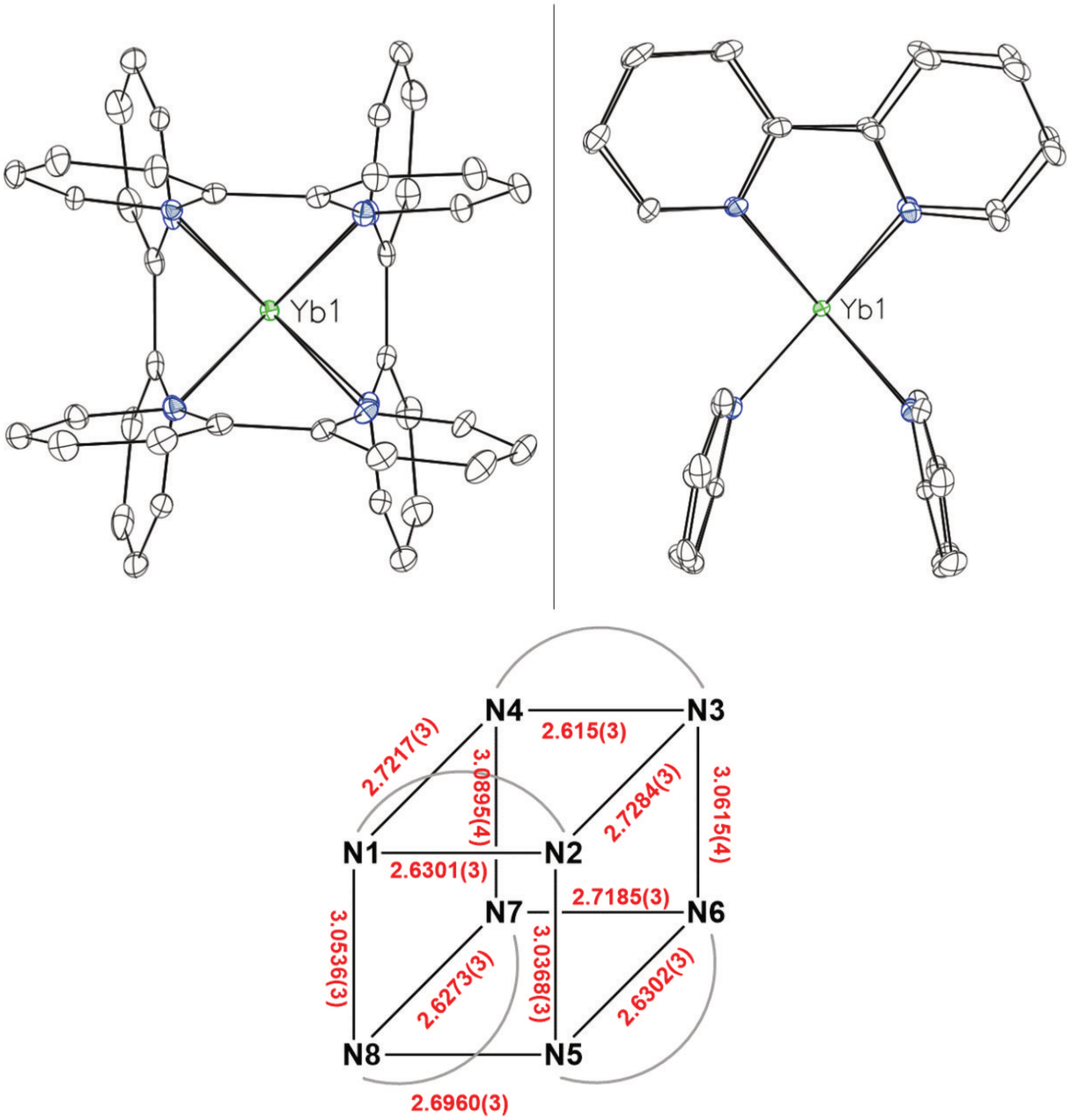

Figure 13. Top: two views of the anion $[Yb(bipy)_4]^{1-}$, **9**, showing the bending of adjacent planes of bipy ligands toward each other. Bottom: schematic representation of **9** with nitrogen atoms superimposed onto the corners of a cube and curved lines representing the rings formed by the bipy ligands. N–N interatomic distances (Å) are shown in red.

chelate. While this appears to be the first example of a structurally characterized $[K_2(18\text{-c-}6)_2Cp^*]^+$ inverse sandwich complex, this motif is established for other cyclopentadienyl anions,[67–71] which suggests that there is a substantial driving force to form these cations in reductions of metal complexes binding cyclopentadienyl ligands.

Conclusions

Exploration of the reduction chemistry of bis(pentamethylcyclopentadienyl) lanthanide bipyridyl complexes has revealed a diversity of reaction types that have led to unusual compositions and structural features. Attempts to further reduce these complexes with potassium and investigation of the reduction chemistry of the bipy anions has repeatedly led to unexpected products. One recurring aspect of these reactions is the formation of mono-Cp* compounds.

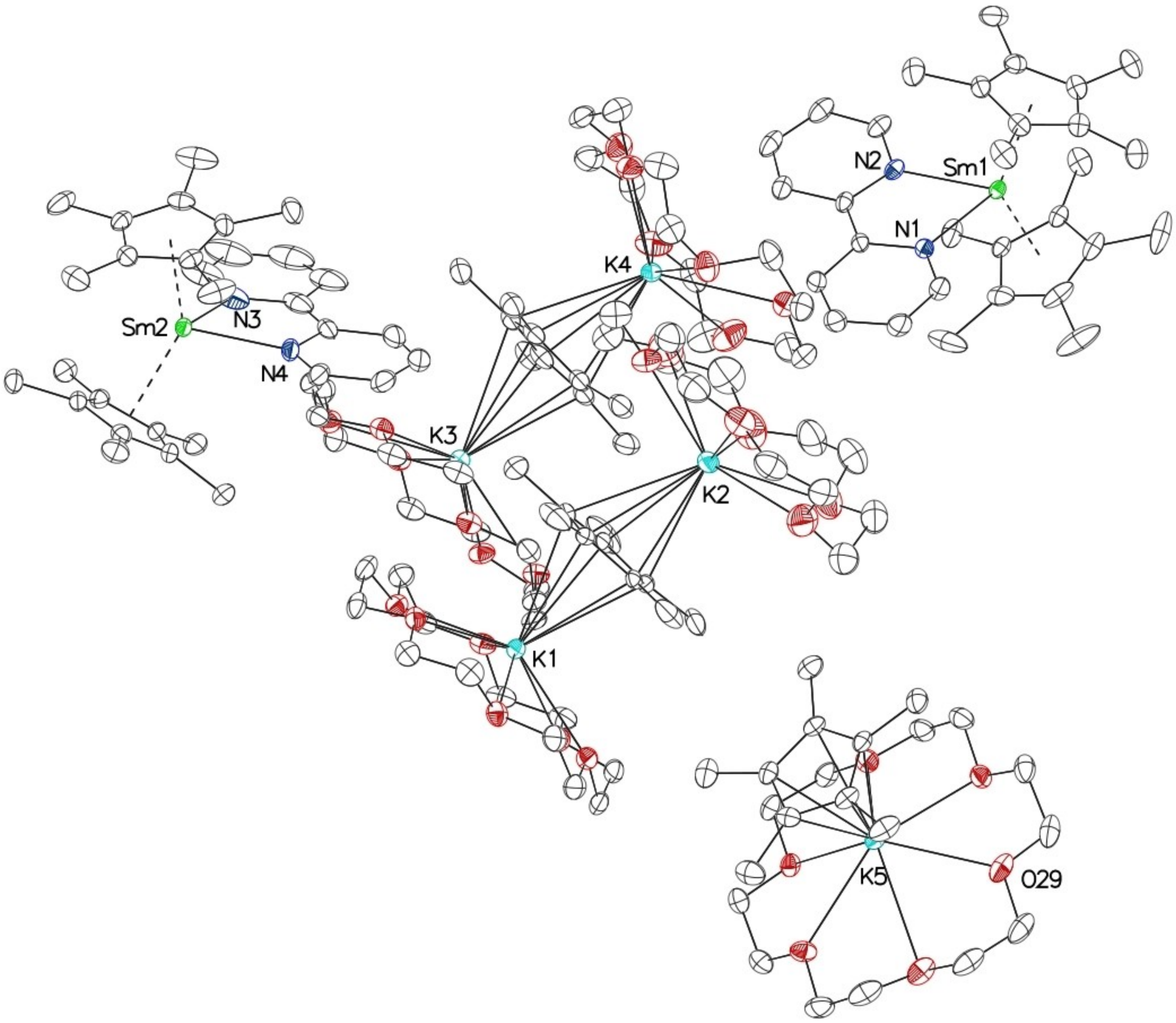

Figure 14. The molecular structure of $[K_2(18\text{-c-}6)_2Cp^*]_2[Cp^*_2Sm(bipy)]_2 \cdot [K(18\text{-c-}6)Cp^*]$, **10**, with thermal ellipsoids drawn at 30 % probability. For clarity, hydrogen atoms and modelled disorder at the bipy ligand bound to Sm2 and the crown ether bound to K2 are not shown.

Isolation of $[K(crypt)]_2[Cp^*Nd(bipy)_2]$, **1**, $Cp^*Lu(bipy)_2$, **3**, $[K(crypt)]_2[Cp^*Eu(THF)(PhNNPh)]_2$, **4**, $[K(crypt)][Cp^*Eu(THF)(PhNNPh)]_2$, **5**, $[K(crypt)]_2[Cp^*Yb(N_3)_4]$, **6**, $[K(crypt)]_2[Cp^*Yb(N_3)_2(bipy)]$, **7 a**, $[K(crypt)]_2[Cp^*Yb(N_3)_2(N_2C_{10}H_7SiMe_3)]$, **7 b**, $[K(crypt)]_2[Cp^*Yb(S_4)(S_5)]$, **8 a**, and $[Cp^*Yb(S_4)_2]^{2-}$, **8 b**, indicates that bipyridyl metallocene complexes can provide access to this less studied area of Cp* lanthanide chemistry. The isolation of $[K(18\text{-c-}6)(THF)][Yb(bipy)_4]$, **9**, from $Cp^*_2Yb(bipy)$ shows that in some cases both Cp* ligands can be lost. The connection between the reactivity of bipy anions and the loss of Cp* is not clear due to the diversity and complexity of these reactions which are typically not stoichiometrically simple. Although the reactions are complicated, they demonstrate the existence of these new compositions and add to the diversity of reactivity available through 2,2′-bipyridine.

Experimental Section

General Considerations

All manipulations were performed by using modified Schlenk techniques or in a Vacuum/Atmospheres glovebox under argon. Solvents were degassed by sparging with dry argon before drying and collection using an S2 Grubbs-type[72] solvent purification system (JC Meyer). All physical measurements were recorded under strictly anaerobic and anhydrous conditions. Infrared spectra were recorded on compressed solid samples using an Agilent Cary 630 ATR/FTIR instrument. ^1H and ^{13}C NMR spectra were recorded using a Bruker AVANCE 500 MHz spectrometer at 298 K unless otherwise stated and referenced to residual solvent signals. Magnetic moments were determined by Evans' method and corrected using the appropriate diamagnetic constants.[73–75] EPR spectra were recorded at the indicated temperature using a Bruker EMX spectrometer equipped with an ER041Xg microwave bridge and externally calibrated with DPPH (g = 2.0036). The EPR spectrum of **3** was fitted using EasySpin.[76] Anhydrous lanthanide chlorides were prepared by treatment of their corresponding hydrates with ammonium chloride as previously described.[77] KCp* was prepared by treatment of HC_5Me_5 with $KN(SiMe_3)_2$ in toluene.[78] Cp*$_2$Sm(bipy),[79] Cp*$_2$Yb(bipy),[24] Cp*$_2$Eu(THF)$_2$,[80] and K/KI (4.3 %, wt.)[81] were prepared according to literature procedures. 2,2′-Bipyridine was purified by sublimation prior to use.

Synthesis of [K(crypt)]$_2$[Cp*Nd(bipy)$_2$], 1, and [K(crypt)][Cp*$_2$NdCl$_2$], 2

Cp*$_2$NdCl(bipy) (0.10 g, 0.16 mmol) and [2.2.2]cryptand (0.120 g, 0.32 mmol) were dissolved in ca. 5 mL of tetrahydrofuran. KC_8 (0.045 g, 0.32 mmol) was then added to this red solution in one portion with stirring at ambient temperature. The mixture immediately became dark brown and stirring was continued overnight. The mixture was then centrifuged and the supernatant was filtered through a pipette packed with ca. 1 cm of filter paper. The dark brown solution was then deposited beneath ca. 3 mL of hexane in a 20 mL vial and the layers were allowed to stand overnight to afford a large crop (0.16 g) of crystalline material, from which dark brown/red crystals of [K(crypt)]$_2$[Cp*Nd(bipy)$_2$]·2THF (**1·THF**) and pale blue crystals of [K(crypt)][Cp*$_2$NdCl$_2$]·THF (**2·THF**) were selected for study by X-ray diffraction. The crystalline material was washed with hexane and residual volatiles were then removed under reduced pressure. ^{1}H NMR spectroscopy of this mixture indicated that **1** and **2** were formed in an approximate 1 : 1 ratio. Thus, considering the total mass of the mixture, **1** and **2** were each formed in an approximate yield of 74 %. ^{1}H NMR of [K(crypt)]$_2$[Cp*Nd(bipy)$_2$], **1**, (500 MHz, THF-D$_8$, 298 K): $\delta = 15.01$ (s, br, 1H, CH (bipy)), 9.54 (d, 2H, CH (bipy), 8.87 (s, br, 2H, CH (bipy), 8.04 (s, 15H, CH_3 (Cp*)), 4.70 (s, 24H, CH_2 (crypt, coincident with corresponding signal of **2**)), 3.77 (s, 24H, CH_2 (crypt, coincident with corresponding signal of **2**)), 3.49 (s, br, 2H, CH (bipy)), 2.90 (s, br, 2H, CH (bipy)), 1.99 (s, 2H, CH (bipy)), −9.43 (s, 2H, CH (bipy)), −21.86 (s, br, 1H, CH (bipy)), −47.11 (s, br, 2H, CH (bipy)). ^{1}H NMR of [K(crypt)][Cp*$_2$NdCl$_2$] (**2**) (500 MHz, THF-D$_8$, 298 K): $\delta = 4.70$ (s, 12H, CH_2 (crypt, coincident with corresponding signal of **1**)), 3.77 (s, 12H, CH_2 (crypt, coincident with corresponding signal of **1**)), 3.72 (s, 12H, CH_2 (crypt, coincident with corresponding signal of **1**), 2.71 (s, 30H, CH_3 (Cp*)).

Alternate synthesis of [K(crypt)][Cp*$_2$NdCl$_2$], 2

Anhydrous $NdCl_3$ (0.072 g, 0.29 mmol), KCp* (0.100 g, 0.57 mmol), and [2.2.2]cryptand (0.11 g, 0.29 mmol) were combined in a 20 mL vial. Tetrahydrofuran (ca. 10 mL) was then added to the stirred mixture, which immediately became yellow. The mixture was stirred overnight, after which time the mixture had become pale blue in color. The mixture was then centrifuged and the supernatant was filtered through a pipette packed with ca. 1 cm of filter paper. The solvent was then removed from the filtrate to give a small amount of pale blue crystals. The pellet in the centrifuge tube was extracted 3 times in ca. 5 mL THF to collect all of the remaining pale blue solid, and the extracts were filtered as above and combined. The solvent was then completely removed from the filtrate and the pale blue residue was combined with the crystalline material. The pale blue material was then washed 3 times with ca. 5 mL portions of hexane to afford 0.20 g (0.22 mmol, 76 %) of [K(crypt)][Cp*$_2$NdCl$_2$] as a pale blue powder. ^{1}H NMR (500 MHz, THF-D$_8$, 298 K): 8.04 (s, br, 30H, CH_3 (Cp*)), 2.23 (s, 24 H, CH_2 (crypt)), 1.38 (s, 12H, CH_2 (crypt)).

Synthesis of Cp*Lu(bipy)$_2$, 3

$LuCl_3$ (0.10 g, 0.36 mmol), 2,2′-bipyridine (0.056 g, 0.36 mmol), and KCp* (0.12 g, 0.71 mmol) were combined in a 20 mL vial. Tetrahydrofuran (ca. 10 mL) was added and the mixture was stirred, whereupon it immediately became orange. 4.3 % wt. K/KI (0.39 g, 0.43 mmol) was then added in one portion to the stirred mixture, which became dark green/brown over ten minutes. The mixture was stirred overnight. After, the solvent was removed under reduced pressure and the solid residue was extracted in ca. 5 mL of hexane. The mixture was centrifuged and the supernatant was filtered. The solvent was then removed slowly from the filtrate under reduced pressure until small, dark brown crystals formed which were suitable for study by X-ray diffraction. Complete removal of the solvent under reduced pressure afforded 0.070 g (0.11 mmol, 31 %) of Cp*Lu(bipy)$_2$, **3**, as a dark brown, microcrystalline solid. ^{1}H NMR (550 MHz, C_6D_6, 298 K): broad signals of low intensity were observed at 4.67 and 3.16 ppm.

Synthesis of [K(crypt)]$_2$[Cp*Eu(THF)(PhNNPh)]$_2$, 4

[K(crypt)][Cp*$_2$Eu(bipy)] (0.20 g, 0.20 mmol) was dissolved in ca. 4 mL of THF to give a dark red/violet solution. Solid azobenzene (0.037 g, 0.20 mmol) was then added in one portion to this solution with stirring. The solution immediately became dark brown/orange in color and was stirred for 18 h. After, the solvent was removed from the solution under reduced pressure to afford a sticky brown residue. The residue was washed 3 times with ca. 3 mL portions of hexane. The residue was then extracted in ca. 2 mL of THF and the solution was filtered through a glass pipette packed with ca. 1 cm of filter paper into a 20 mL vial. Hexane (ca. 2 mL) was then layered on top of this solution and the vial was sealed and allowed to stand for 24 hours at ambient temperature, whereupon a small amount of orange/brown crystals of **4** which were suitable for study by X-ray diffraction had grown on the walls of the vial.

Synthesis of [K(crypt)][Cp*Eu(THF)(PhNNPh)]$_2$, 5

Azobenzene (0.081 g, 0.44 mmol), [2.2.2] cryptand (0.17 g, 0.44 mmol), and K/KI (0.44 g, 4.3 wt. %, 0.49 mmol) were combined in a 20 mL vial and ca. 10 mL THF was added with stirring to give a dark violet colored mixture. Cp*$_2$Eu(THF)$_2$ was then added to this mixture in one portion and the mixture immediately became dark brown in color. The mixture was stirred for ca. 18 h. After, the mixture was centrifuged, the supernatant was filtered through a glass pipette packed with ca. 1 cm of filter paper, and the solvent was removed from the filtrate under reduced pressure to give a sticky brown residue. The residue was washed 3 times with ca. 2 mL portions of hexane. Residual volatiles were removed from the residue under reduced pressure. The residue was then dissolved in ca. 4 mL THF in a 20 mL vial. The vial was then sealed and stored at ca. −35 °C for ca. 18 h. to afford a small amount of dark brown crystals of **5** which were suitable for study by X-ray diffraction.

Synthesis of [K(crypt)]$_2$[Cp*Yb(N$_3$)$_4$], 6

[K(crypt)][Cp*$_2$Yb(bipy)] (0.10 g, 0.10 mmol) was dissolved in ca. 3 mL THF in a 20 mL vial to give a dark red/violet solution. Trimethylsilylazide (0.090 g, 0.79 mmol) was then added to this solution in one portion with stirring and the solution immediately became brown in color. The brown solution was then filtered through a glass pipette packed with ca. 1 cm of filter paper and deposited beneath ca. 3 mL of diethyl ether in a 20 mL vial. The vial was then sealed and allowed to stand for ca. 24 h. at ambient temperature whereupon a small amount of red crystals had grown which were suitable for study by X-ray diffraction.

Synthesis of [K(crypt)]$_2$[Cp*Yb(N$_3$)$_2$(bipy)], 7a, and [K(crypt)]$_2$[Cp*Yb(N$_3$)$_2$(N$_2$C$_{10}$H$_7$SiMe$_3$)], 7b. [K(crypt)][Cp*$_2$Yb(bipy)] (0.10 g, 0.10 mmol) was dissolved in ca. 3 mL THF in a 20 mL vial to give a dark red/violet solution. Trimethylsilylazide (0.010 g, 0.10 mmol) was then added to this solution in one portion with stirring. The solution was then stirred for ca. 18 h., after which time it had become brown in color. The solution was filtered through a glass pipette packed with ca. 1 cm. of filter paper and deposited beneath ca. 3 mL of diethyl ether in a 20 mL vial. The vial was then sealed and allowed to stand for ca. 24 h. at ambient temperature, whereupon a small amount of dark red crystals had grown which were suitable for study by X-ray diffraction.

Synthesis of $[\mathrm{K(crypt)}]_2[\mathrm{Cp^*Yb(S_4)(S_5)}]$, 8 a, and $[\mathrm{K(crypt)}]_2[\mathrm{Cp^*Yb(S_4)_2}]$, 8 b

$[\mathrm{K(crypt)}][\mathrm{Cp^*_2Yb(bipy)}]$ (0.20 g, 0.20 mmol) was dissolved in ca. 10 mL of THF to give a dark red/violet solution. Sulfur (0.032 g, 1.0 mmol) was then added to this solution in one portion with stirring. The solution immediately became red and was stirred for 1 h. The solvent was then removed under reduced pressure to give a sticky brown residue. The residue was washed 3 times with 3 mL portions of hexane. Residual volatiles were then removed from the residue under reduced pressure, and the brown powder was dissolved in ca. 4 mL of THF. The red solution was then filtered through a glass pipette packed with ca. 1 cm of filter paper and deposited beneath ca. 2 mL of hexane in a 20 mL vial. The vial was then sealed and allowed to stand at ambient temperature for ca. 18 h., whereupon a small amount of red crystals of $[\mathrm{K(crypt)}]_2[\mathrm{Cp^*Yb(S_4)(S_{4/5})}]$, **8**, had grown which were suitable for study by X-ray diffraction.

Synthesis of $[\mathrm{K(18\text{-}crown\text{-}6)}][\mathrm{Yb(bipy)_4}]$, 9

$\mathrm{Cp^*_2Yb(bipy)}$ (0.68 g, 1.13 mmol) and 18-crown-6 (0.30 g, 1.13 mmol) were combined in a 20 mL vial and ca. 10 mL THF was added to give a dark orange/brown solution. $\mathrm{KC_8}$ (0.17 g, 1.25 mmol) was then added to this solution in one portion. The mixture immediately became dark violet in color and was stirred overnight. The mixture was then centrifuged and the supernatant was filtered and deposited beneath ca. 3 mL hexane in a 20 mL vial. The vial was sealed and stored at ambient temperature. After overnight storage, a small amount of dark violet crystals of $[\mathrm{K(18\text{-}crown\text{-}6)}][\mathrm{Yb(bipy)_4}]$, **9**, had grown which were suitable for study by X-ray diffraction.

Synthesis of $[\mathrm{K_2(18\text{-}c\text{-}6)_2Cp^*}][\mathrm{Cp^*_2Sm(bipy)}]_2\cdot[\mathrm{K(18\text{-}c\text{-}6)Cp^*}]$, 10

$\mathrm{Cp^*_2Sm(bipy)}$ (0.30 g, 0.52 mmol) and 18-crown-6 (0.41 g, 1.6 mmol) were dissolved in ca. 10 mL of tetrahydrofuran to give a dark orange/brown solution. $\mathrm{KC_8}$ (0.15 g, 1.1 mmol) was then added to this solution with stirring. The brown mixture was then stirred for ca. 18 hours at ambient temperature. After, the mixture was centrifuged and the supernatant was filtered through a glass pipette packed with ca. 1 cm of filter paper. The solvent was removed from the filtrate under reduced pressure to give a sticky brown residue. The residue was washed 3 times with ca. 3 mL portions of hexane and residual volatiles were removed from the solid residue under reduced pressure. The brown residue was then dissolved in ca. 5 mL of THF, filtered through a glass pipette packed with ca. 1 cm of filter paper, and the solution was deposited beneath ca. 3 mL of hexane in a 20 mL vial. The vial was allowed to stand at ambient temperature for ca. 18 h. after which time a small amount of brown crystals of $[\mathrm{K_2(18\text{-}c\text{-}6)_2Cp^*}][\mathrm{Cp^*_2Sm(bipy)}]_2\cdot[\mathrm{K(18\text{-}c\text{-}6)Cp^*}]$, **10**, had grown which were suitable for study by X-ray diffraction.

Supporting Information

The Supporting Information, including spectra (NMR, infrared, UV-Vis), crystallographic data, and photographs of material is available free of charge at https://doi.org/10.1002/ejic.202300732. CCDC entries 2190108 (**1**), 2190421 (**2**), 2191917 (**3**), 2213073 (**4**), 2233288 (**5**), 2307323 (**6**), 2307324 (**7**), 2307261 (**8**), 2282191 (**9**), and 2307322 (**10**) contain the supplementary crystallographic data of the complexes described here. These data can be obtained free of charge via www.ccdc.cam.ac.uk/data_request/cif, by emailing data request@ccdc.cam.ac.uk, or by contacting The Cambridge Crystallographic Data Centre, 12 Union Road, Cambridge CB2 1EZ, UK; fax: +44 1223 336033.

Acknowledgements

The authors wish to acknowledge the US National Science Foundation (CHE-2154255) for support of this work and Dr. Joshua D. Queen for providing the fitted EPR spectrum of complex **3**.

Conflict of Interests

The authors declare no competing financial interest.

Data Availability Statement

The data that support the findings of this study are available in the supplementary material of this article.

[1] V. Lyaskovskyy, B. de Bruin, *ACS Catal.* **2012**, *2*, 270–279.
[2] K. Ray, T. Petrenko, K. Wieghardt, F. Neese, *Dalton Trans.* **2007**, *No. 16*, 1552–1566.
[3] J. I. van der Vlugt, J. N. H. Reek, *Angew. Chem. Int. Ed.* **2009**, *48*, 8832–8846.
[4] E. J. Coughlin, M. Zeller, S. C. Bart, *Angew. Chem. Int. Ed.* **2017**, *56*, 12142–12145.
[5] C. Camp, V. Guidal, B. Biswas, J. Pécaut, L. Dubois, M. Mazzanti, *Chem. Sci.* **2012**, *3*, 2433–2448.
[6] E. J. Schelter, R. Wu, B. L. Scott, J. D. Thompson, T. Cantat, K. D. John, E. R. Batista, D. E. Morris, J. L. Kiplinger, *Inorg. Chem.* **2010**, *49*, 924–933.
[7] N. Jori, M. Falcone, R. Scopelliti, M. Mazzanti, *Organometallics* **2020**, *39*, 1590–1601.
[8] S. J. Kraft, U. J. Williams, S. R. Daly, E. J. Schelter, S. A. Kozimor, K. S. Boland, J. M. Kikkawa, W. P. Forrest, C. N. Christensen, D. E. Schwarz, P. E. Fanwick, D. L. Clark, S. D. Conradson, S. C. Bart, *Inorg. Chem.* **2011**, *50*, 9838–9848.
[9] D. P. Cladis, J. J. Kiernicki, P. E. Fanwick, S. C. Bart, *Chem. Commun.* **2013**, *49*, 4169–4171.
[10] S. Herzog, G. Byhan, P. Wulfert, *Z. Chem.* **1961**, *1*, 370–371.
[11] G. R. Feistel, T. P. Mathai, *J. Am. Chem. Soc.* **1968**, *90*, 2988–2989.
[12] S. Herzog, R. Schuster, *Z. Chem.* **1967**, *7*, 26–27.
[13] S. Herzog, K. Gustav, *Z. Anorg. Allg. Chem.* **1966**, *346*, 162–165.
[14] M. N. Bochkarev, B. I. Petrov, I. L. Fedyushkin, T. V. Petrovskaya, V. I. Nevodchikov, N. B. Patrikeeva, L. N. Zakharov, Y. T. Strucchkov, *Russ. Chem. Bull.* **1997**, *46*, 371–373.
[15] I. L. Fedushkin, T. V. Petrovskaya, F. Girgsdies, V. I. Nevodchikov, R. Weimann, H. Schumann, M. N. Bochkarev, *Russ. Chem. Bull.* **2000**, *49*, 1869–1876.
[16] Y. Xiao, R. Sun, J. Liang, Y. Fang, Z. Liu, S. Jiang, B. Wang, S. Gao, W. Huang, *Inorg. Chem. Front.* **2021**, *8*, 2591–2602.

[17] W. Ren, G. Zi, M. D. Walter, *Organometallics* **2012**, *31*, 672–679.
[18] P. Yang, E. Zhou, B. Fang, G. Hou, G. Zi, M. D. Walter, *Organometallics* **2016**, *35*, 2129–2139.
[19] S. Wang, D. Wang, T. Li, Y. Heng, G. Hou, G. Zi, M. D. Walter, *Organometallics* **2022**, *41*, 1543–1557.
[20] G. Zi, L. Jia, E. L. Werkema, M. D. Walter, J. P. Gottfriedsen, R. A. Andersen, *Organometallics* **2005**, *24*, 4251–4264.
[21] C. N. Carlson, C. J. Kuehl, L. Ogallo, D. A. Shultz, J. D. Thompson, M. L. Kirk, R. L. Martin, K. D. John, D. E. Morris, *Organometallics* **2007**, *26*, 4234–4242.
[22] J. M. Veauthier, E. J. Schelter, C. N. Carlson, B. L. Scott, R. E. Da Re, J. D. Thompson, J. L. Kiplinger, D. E. Morris, K. D. John, *Inorg. Chem.* **2008**, *47*, 5841–5849.
[23] C. R. Stennett, J. Q. Nguyen, J. W. Ziller, W. J. Evans, *Organometallics* **2023**, *42*, 696–707.
[24] M. Schultz, J. M. Boncella, D. J. Berg, T. D. Tilley, R. A. Andersen, *Organometallics* **2002**, *21*, 460–472.
[25] S. Arndt, J. Okuda, *Chem. Rev.* **2002**, *102*, 1953–1976.
[26] W. J. Evans, J. M. Perotti, S. A. Kozimor, T. M. Champagne, B. L. Davis, G. W. Nyce, C. H. Fujimoto, R. D. Clark, M. A. Johnston, J. W. Ziller, *Organometallics* **2005**, *24*, 3916–3931.
[27] M. R. MacDonald, J. W. Ziller, W. J. Evans, *Inorg. Chem.* **2011**, *50*, 4092–4106.
[28] B. M. Schmiege, J. W. Ziller, W. J. Evans, *Inorg. Chem.* **2010**, *49*, 10506–10511.
[29] W. J. Evans, D. S. Lee, J. W. Ziller, N. Kaltsoyannis, *J. Am. Chem. Soc.* **2006**, *128*, 14176–14184.
[30] H. Schumann, I. Albrecht, J. Loebel, E. Hahn, M. B. Hossain, D. Van der Helm, *Organometallics* **1986**, *5*, 1296–1304.
[31] M. D. Rausch, K. J. Moriarty, J. L. Atwood, J. A. Weeks, W. E. Hunter, H. G. Brittain, *Organometallics* **1986**, *5*, 1281–1283.
[32] W. J. Evans, J. M. Olofson, H. Zhang, J. L. Atwood, *Organometallics* **1988**, *7*, 629–633.
[33] Y.-H. Lin, D.-S. Zeng, Q. Shen, *Gov. Rep. Announce.* **1995**.
[34] M. T. Gamer, G. Canseco-Melchor, P. W. Roesky, *Z. Anorg. Allg. Chem.* **2003**, *629*, 2113–2116.
[35] P. C. Junk, M. K. Smith, *Appl. Organomet. Chem.* **2004**, *18*, 252.
[36] P. L. Watson, J. F. Whitney, R. L. Harlow, *Inorg. Chem.* **1981**, *20*, 3271–3278.
[37] J. O. Rothbaum, A. Motta, Y. Kratish, T. J. Marks, *J. Am. Chem. Soc.* **2022**, *144*, 17086–17096.
[38] J. C. Wedal, C. J. Windorff, D. N. Huh, A. J. Ryan, J. W. Ziller, W. J. Evans, *J. Coord. Chem.* **2021**, *74*, 74–91.
[39] C. C. Scarborough, K. Wieghardt, *Inorg. Chem.* **2011**, *50*, 9773–9793.
[40] A. W. Addison, T. N. Rao, J. Reedijk, J. van Rijn, G. C. Verschoor, *J. Chem. Soc. Dalton Trans.* **1984**, *No. 7*, 1349–1356.
[41] T. Scheiring, A. Klein, W. Kaim, *J. Chem. Soc. Perkin Trans. 2* **1997**, *No. 12*, 2569–2572.
[42] W. Kaim, S. Kohlmann, *Chem. Phys. Lett.* **1987**, *139*, 365–369.
[43] B. Li, B. L. Geoghegan, C. Wölper, G. E. I. I. I. Cutsail, S. Schulz, *ACS Omega* **2021**, *6*, 18325–18332.
[44] R. G. Belli, V. C. Tafuri, N. A. Garcia, C. C. Roberts, *Organometallics* **2023**, *42*, 1059–1064.
[45] M. N. Bochkarev, I. L. Fedushkin, V. I. Nevodchikov, V. K. Cherkasov, H. Schumann, H. Hemling, R. Weimann, *J. Organomet. Chem.* **1996**, *524*, 125–131.
[46] A. Bondi, *J. Phys. Chem.* **1964**, *68*, 441–451.
[47] R. L. Halbach, G. Nocton, J. I. Amaro-Estrada, L. Maron, C. H. Booth, R. A. Andersen, *Inorg. Chem.* **2019**, *58*, 12083–12098.
[48] W. J. Evans, G. W. Nyce, R. D. Clark, R. J. Doedens, J. W. Ziller, *Angew. Chem. Int. Ed.* **1999**, *38*, 1801–1803.
[49] R. R. Langeslay, G. P. Chen, C. J. Windorff, A. K. Chan, J. W. Ziller, F. Furche, W. J. Evans, *J. Am. Chem. Soc.* **2017**, *139*, 3387–3398.
[50] T. D. Tilley, R. A. Andersen, B. Spencer, H. Ruben, A. Zalkin, D. H. Templeton, *Inorg. Chem.* **1980**, *19*, 2999–3003.
[51] W. J. Evans, D. K. Drummond, L. R. Chamberlain, R. J. Doedens, S. G. Bott, H. Zhang, J. L. Atwood, *J. Am. Chem. Soc.* **1988**, *110*, 4983–4994.
[52] R. D. Shannon, *Acta Crystallogr. Sect. A* **1976**, *32*, 751–767.
[53] M. E. Fieser, M. R. MacDonald, B. T. Krull, J. E. Bates, J. W. Ziller, F. Furche, W. Evans, J *J. Am. Chem. Soc.* **2015**, *137*, 369–382.
[54] M. B. Robin, P. Day, Mixed Valence Chemistry-A Survey and Classification; H. J. Emeléus, A. G. Sharpe, Eds.; in *Advances in Inorganic Chemistry and Radiochemistry*. Academic Press, 1968; Vol. 10, pp 247–422.
[55] L. A. Solola, A. V. Zabula, W. L. Dorfner, B. C. Manor, P. J. Carroll, E. J. Schelter, *J. Am. Chem. Soc.* **2017**, *139*, 2435–2442.
[56] T. E. Rieser, R. Thim-Spöring, D. Schädle, P. Sirsch, R. Litlabø, K. W. Törnroos, C. Maichle-Mössmer, R. Anwander, *J. Am. Chem. Soc.* **2022**, *144*, 4102–4113.
[57] K. Rosenstengel, A. Schulz, O. Niehaus, O. Janka, R. Pöttgen, A. Villinger, *Eur. J. Inorg. Chem.* **2018**, *2018*, 778–790.
[58] Z.-J. Lv, Z. Chai, M. Zhu, J. Wei, W.-X. Zhang, *J. Am. Chem. Soc.* **2021**, *143*, 9151–9161.
[59] T. Kauffmann, J. König, A. Woltermann, *Chem. Ber.* **1976**, *109*, 3864–3868.
[60] Y. Gu, Y. Shen, C. Zarate, R. Martin, *J. Am. Chem. Soc.* **2019**, *141*, 127–132.
[61] N.-N. Li, M. Li, J.-N. Gao, Z. Zhang, J.-B. Xie, *J. Org. Chem.* **2022**, *87*, 10876–10889.
[62] C. Cheng, J. F. Hartwig, *Chem. Rev.* **2015**, *115*, 8946–8975.
[63] Y.-Z. Ma, S. Bestgen, M. T. Gamer, S. N. Konchenko, P. W. Roesky, *Angew. Chem. Int. Ed.* **2017**, *56*, 13249–13252.
[64] M. Herberhold, G.-X. Jin, W. Milius, *Angew. Chem. Int. Ed. Engl.* **1993**, *32*, 85–87.
[65] W. Bubenheim, U. Müller, *Z. Anorg. Allg. Chem.* **1994**, *620*, 1607–1612.
[66] S. Fortier, J. Veleta, A. Pialat, J. Le Roy, K. B. Ghiassi, M. M. Olmstead, A. Metta-Magaña, M. Murugesu, D. Villagrán, *Chem. Eur. J.* **2016**, *22*, 1931–1936.
[67] W. W. Brennessel, J. E. Ellis, *Inorg. Chem.* **2012**, *51*, 9076–9094.
[68] M. R. MacDonald, J. E. Bates, J. W. Ziller, F. Furche, W. J. Evans, *J. Am. Chem. Soc.* **2013**, *135*, 9857–9868.
[69] R. Zitz, H. Arp, J. Hlina, M. Walewska, C. Marschner, T. Szilvási, B. Blom, J. Baumgartner, *Inorg. Chem.* **2015**, *54*, 3306–3315.
[70] D. N. Huh, J. W. Ziller, W. J. Evans, *Dalton Trans.* **2018**, *47*, 17285–17290.
[71] J.-C. Berthet, C. Villiers, J.-F. Le Maréchal, B. Delavaux-Nicot, M. Lance, M. Nierlich, J. Vigner, M. Ephritikhine, *J. Organomet. Chem.* **1992**, *440*, 53–65.
[72] A. B. Pangborn, M. A. Giardello, R. H. Grubbs, R. K. Rosen, F. J. Timmers, *Organometallics* **1996**, *15*, 1518–1520.
[73] D. F. Evans, *J. Chem. Soc.* **1959**, *No. 0*, 2003–2005.
[74] S. K. Sur, *J. Magn. Reson.* **1989**, *82*, 169–173.
[75] G. A. Bain, J. F. Berry, *J. Chem. Educ.* **2008**, *85*, 532.
[76] S. Stoll, A. Schweiger, *J. Magn. Reson.* **2006**, *178*, 42–55.
[77] G. Meyer, E. Garcia, J. D. Corbett, *Inorg. Synth.* **1989**, *26*, 146–150.
[78] J. C. Wedal, J. W. Ziller, F. Furche, W. J. Evans, *Inorg. Chem.* **2022**, *61*, 7365–7376.
[79] W. J. Evans, D. K. Drummond, *J. Am. Chem. Soc.* **1989**, *111*, 3329–3335.
[80] P. L. Watson, T. H. Tulip, I. Williams, *Organometallics* **1990**, *9*, 1999–2009.
[81] J. Hicks, M. Juckel, A. Paparo, D. Dange, C. Jones, *Organometallics* **2018**, *37*, 4810–4813.

Manuscript received: December 2, 2023
Revised manuscript received: February 6, 2024
Version of record online: March 7, 2024